

**ACCURACY EVALUATION OF INTRA-ORAL OPTICAL IMPRESSIONS: A NOVEL
APPROACH**

Mohammad A. Atieh

A thesis submitted to the faculty at the University of North Carolina at Chapel Hill in partial fulfillment of the requirements for the degree of Master of Science in the School of Dentistry
(Operative Dentistry)

Chapel Hill
2016

Approved by:

Ibrahim Duqum

André Ritter

Ching-Chang Ko

© 2016
Mohammad A. Atieh
ALL RIGHTS RESERVED

ABSTRACT

Mohammad A. Atieh: Accuracy Evaluation of Intra-Oral Optical Impressions: A Novel Approach
(Under the direction of Ibrahim Duqum)

Objective: To compare the accuracy (trueness and precision) of optical and conventional impressions in-vivo.

Materials and Methods: Five study participants were consented and enrolled. For each participant, optical (*CEREC® Omnicam; Dentsply Sirona, Charlotte, USA*) and conventional (*vinylsiloxanether; Identium®, Kettenbach, Huntington Beach, USA*) impressions of a custom-made intra-oral Co-Cr alloy reference appliance fitted to the mandibular arch were obtained. 3D digital models were created for stone models obtained from the conventional impression group and for the reference appliances using a validated high accuracy reference scanner (*Infinite focus standard; Alicona Corporation, Bartlett, USA*). For the optical impression group, 3D digital models were obtained directly from the intraoral scans. Total mean trueness of each impression system was calculated by superimposing the 3D models and averaging the mean absolute deviations of the impression replicates from their 3D reference model for each participant followed by averaging the obtained values across all participants. Total mean precision for each impression system was calculated by superimposing the 3D models and averaging the mean absolute deviations between all the impression replicates for each participant (10 pairs) followed by averaging the obtained values across all participants. Data were analyzed using repeated measures ANOVA at a 0.05 significance level.

Results: Optical impressions had significantly lower mean trueness and precision ($46.2 \pm 11.4 \mu\text{m}$ and $61.1 \pm 4.9 \mu\text{m}$, respectively) than those for conventional impressions ($17.0 \pm 6.6 \mu\text{m}$ and $16.9 \pm 5.8 \mu\text{m}$ respectively), suggesting higher accuracy for conventional impressions.

Conclusions: Within the limitations of this study, full-arch (first molar-first molar) optical impressions are less accurate than conventional impressions, but might exhibit enough accuracy for quadrant impressions.

To my great father and mother whose love and support were endless.

To my wonderful wife Melanie whose love and dedication were unimaginable.

To my beautiful daughter Mariam who brought the joy to my life.

ACKNOWLEDGEMENTS

I would like to thank my mentor and my great friend Dr. Ibrahim Duqum for all his time and effort in guiding me through this research.

I would like to thank my committee members Dr. André Ritter and Dr. Ching-Chang Ko for their valuable suggestions and their help in completing this research.

I would like to thank *Dentsply Sirona USA* for facilitating this project by providing the Cerec® Omnicam and the technical support needed.

I would like to thank *Kettenbach USA and Dentsply USA* for donating materials needed for this research.

I would like to thank the research participants for volunteering in this project.

TABLE OF CONTENTS

LIST OF TABLES	ix
LIST OF FIGURES	x
LIST OF ABBREVIATIONS	xii
CHAPTER 1: LITERATURE REVIEW	1
1.1 Introduction	1
1.2 Historical background	4
1.3 Scanning technologies of the current intra-oral scanners	4
1.3.1 Active triangulation	5
1.3.2 Parallel Confocal Imaging Technique	10
1.3.3 Optical Coherence tomography	11
1.3.4 Active wavefront sampling	12
1.4 Scanning technologies for IOSs under the stage of development	14
1.4.1 Accordion fringe interferometry	14
1.4.2 Scanner based on Time-of-flight (TOF technology)	15
1.4.3 High frequency ultrasound 3D assisted micro-scanning	15
1.5 Accuracy of intraoral scanners	15
1.6 Intraoral scanning challenges	22
CHAPTER 2: MANUSCRIPT.....	26
2.1 Introduction	26

2.2 Materials and Methods	28
2.2.1 Reference appliance fabrication.....	29
2.2.2 Obtaining impressions	30
2.2.3 Creating reference models (Gold standards).....	31
2.2.4 Measuring deviations from reference models.....	32
2.3 Statistical analysis	33
2.4 Results.....	34
2.5 Discussion	35
2.6 Conclusions	39
2.6 Future direction.....	39
Tables	40
Figures.....	42
References	70

LIST OF TABLES

Table 1 Mean trueness and precision for the conventional and optical impression groups.	40
Table 2 Overall trueness and precision.....	41

LIST OF FIGURES

Figure 1. A zoomed-in view from a molar model showing 3D points connected in a form of triangles.....	42
Figure 2. Omnicam stripe pattern	43
Figure 3. Scheimpflug principle	44
Figure 4. Representation of parallax.....	45
Figure 5. Epipolar plane	46
Figure 6. Coherent and noncoherent lights.....	47
Figure 7. (A)Constructive interference (B) Destructive interference	48
Figure 8. Schematic presentation of the OCT.....	49
Figure 9. Schematic of depth-from-defocus approach.....	50
Figure 10. Static wavefront sampling.....	51
Figure 11. Static two apertures mask in conjunction with a rotating sampling disk	52
Figure 12. Microlense implementation in AWV.	53
Figure 13. Schematic presentation of the Accordion Fringe Interferometry technology.	54
Figure 14. Illustration of phase shift. The horizontal axis represents an angle (phase) that is increasing with time.....	55
Figure 15. A new protocol for evaluating accuracy in-vitro by Guth et al.....	56
Figure 16. Edge effects	57
Figure 17. Illustration of the reference appliance design.....	58
Figure 18. Acrylic reference appliance	59
Figure 19. Wax spacer over a reference appliance before tray fabrication.	60
Figure 20. Co-Cr reference appliance.....	61
Figure 21. A reference appliance in the water bath to bring its temperature close to the oral temperature	62

Figure 22. Conventional impression after excess was removed with scalpel.....	63
Figure 23. A reference appliance powdered and ready fro scan under the reference scanner.....	64
Figure 24. Image field selection before scanning with reference scanner.....	65
Figure 25. A cropped model after removing all the areas outside the field of comparison.....	66
Figure 26. Example of the most common pattern of deviation from each impression system.....	67
Figure 27. Distribution of trueness percentiles	68
Figure 28. Distribution of precision percentiles	69

LIST OF ABBREVIATIONS

3D	Three Dimensional
CAD/CAM	Computer-Aided Design / Computer-Aided-Manufacturing
CAI	Computer-Aided-Impression
Co-Cr	Cobalt-Chromium
DI	Digital Impression
LED	Light Emitting Diode
OIS	Optical Intraoral Scanner
RPD	Removable Partial Denture
VSXE	Vinylsiloxanether

CHAPTER 1: LITERATURE REVIEW

1.1 Introduction

The process of collecting information about the topography of an object in a way to facilitate the construction of a three-dimensional model of that object is referred to as three-dimensional (3D) mapping, surveying or simply 3D scanning. Digital 3D models of dental arches can be obtained in the same way using either direct or indirect approach. Indirect approach involves digitization of conventional impressions or stone models by a dental laboratory scanner. Direct approach involves the use of intraoral scanner to obtain 3D dental model by a process called computer-aided-impression (CAI) or simply digital impression (DI).

Digital impressions have several advantages over conventional impressions that can be summarized in the following:

- There is no dimensional change or susceptibility to damage from handling.
- No trays, tray adhesives and impression material dispensing systems are needed. Also less cost is incurred from the limited shelf-life of impression materials. This could have a huge impact on large dental practices or educational institutions that stock large amounts of impression materials and its armamentarium.
- Electronic transport of the dental impression to the lab. This includes ease of communication and limitation of cost and effort with no cross infection risk.
- Immediate on-screen feedback that permits evaluation of preparation; margin capture and clarity; undercuts, path of withdrawal and occlusal clearance.

- Convenient virtual cutting tool that is available in some of the intraoral scanning systems. This tool enables the operator to cut unclear impression areas and rescan them without the need to repack the cord as it is the case with the conventional impression procedure. This tool can also have extended use at the day of preparation. It enables the operator to save time by cropping out the area of the planned preparation from a previously saved diagnostic impression so to be added later after the preparation is completed (1).
- Difficult cases can be scanned in segments and merged together(1).
- With future technology, there will be no need for tissue retraction. The use of high-frequency ultrasound might enable trans-gingival scanning of the preparation margin(2).
- Fusion option. It allows the superimposition of the DI with scans from other imaging systems like CBCT(1). This opens the possibilities for case planning.
- Superior marginal accuracy, strength and longevity of chairside CAD/CAM provisional restorations compared to conventional ones (3-5). Also the benefits of time saving and the comfort of the patient and the dentist can't be underestimated. Provisional restorations' design and fabrication can be delegated to auxiliary staff while the dentist can provide other procedures to the same patient or other patients.
- The ability to provide chairside definitive restoration at the same appointment. This may result in a superior bond quality to the tooth structure (6, 7).

- Convenient storage and far less space requirement than conventional models especially for diagnostic and planning purposes where no physical models are needed. Moreover, easier retrievability allows more efficient monitoring of tooth wear and gingival level.
- New possibilities in the field of occlusion recording and analysis; however, application of dynamic occlusion might not be available in all the DI systems (1).

On the other hand, DIs have some limitations that can be summarized into the following:

- The size of the scanning wand might make it difficult to scan some areas.
- Time limitation imposed by some systems might be a problem especially in the beginning of the learning curve.
- It is difficult to scan subgingival margins.

Nevertheless, the adoption of DI technology in the daily dental practice and the shift towards complete digital work flow can be only achieved if DIs prove to have a level of accuracy that is comparable to conventional impressions.

The accuracy of dental restorations that are obtained by digital impressions is determined by the accuracy of the whole fabrication chain. The first step of this fabrication chain is represented by the DI. This step will determine the accuracy of the whole system assuming that other factors are held constant. These factors include post-scanning software processing, fabrication processes (e.g. Milling, 3D printing, casting) and post fabrication procedures (e.g. sintering, finishing and polishing). Therefore, evaluating the accuracy of the first step in the dental fabrication chain represented by the DI is mandatory. This should be performed before evaluating the accuracy of the resultant dental restorations.

1.2 Historical background

The CAD/CAM concept in dentistry was introduced by a French dentist, Dr. Fracois Duret in his thesis titled “Empreinte Optique” (Optical Impression) presented at the university of Claude Bernard in France in 1973(8). The system he developed was a complete intraoral scanning and milling system. The intraoral scanner was a laser based scanner that recorded an image of the prepared tooth on a holographic board. The image then was transferred to a computer and eventually to a computer numeric control (CNC) milling machine (9). Patent of this system was obtained in 1984 and followed by first presentation at Chicago Midwinter meeting in 1989 where he fabricated the first chair-side dental crown in four hours (8, 10).

In the meantime, a Swiss dentist, Dr. Werner Mörmann, and an electrical engineer, Marco Brandestini, were developing a system that was then introduced in 1987 as the first commercially available CAD/CAM system in dentistry for fabrication of dental restorations (10). Since then many systems have developed and by the end of 2015 there was around twenty intraoral scanning systems available in the market worldwide.

1.3 Scanning technologies of the current intra-oral scanners

All the current scanners are based on non-contact optical scanning technologies including triangulation, confocal microscopy, optical coherence tomography, photogrammetry, active and passive stereovision, interferometry and phase shift principals(11). These scanning technologies, though new to the dental field, have been applied for many years in the 3D mapping of objects of different sizes ranging from small to mega structures.

Current optical intraoral scanners (OISs) may combine more than one of the aforementioned technologies in addition to other assistive ones in an effort to overcome the

challenging intraoral scanning environment that includes humidity; different optical properties of the scanned surfaces; movement of the scanning wand and the patient(12). Examples of assistive technologies include, mirror warmers that prevent fogging and automatic shake detection mechanism that permits still image acquisition to avoid distortion (8, 12).

OISs use a camera with either a laser or LED light source to detect the surface topography of the intraoral scene. A point cloud that is composed of a set of points that is located in the 3D coordinate system is generated from the scanned data. Software algorithms are then applied to filter out scan outliers and connects the 3D points in a form of triangles to create a tessellated surface in a process called polygonization (Figure 1) (13). The output is stored in STL (**STereoLithography or Standard Tessellation Language**) file format that is readable by dental and non-dental CAD softwares.

1.3.1 Active triangulation

Active triangulation is one of the most popular technologies that is used in the field of 3D scanning. It is grounded on the very basic triangulation principle that uses trigonometry and simple mathematics to measure distance. It is called triangulation because the camera, the light source and the object point that is being viewed form a triangle. Based on a fixed distance between the camera and the light source; a fixed angle of the light source and a measurable viewing angle, a trigonometry is used to calculate the distance between the object and the camera. Active triangulation uses a structured light source and at least one camera compared to passive triangulation that uses multiple cameras and unstructured light (12, 14).

Active triangulation scanners projects structured light pattern (e.g. light stripe or grid pattern) on the surface being scanned. The camera detects the deformation of that pattern and

distance is calculated between each point in the pattern and a reference (15). While the light pattern is moved across the surface being scanned, distances are actively calculated throughout the process that will be converted into point cloud of the scanned surface that forms the basis of the final 3D model.

The light source could be a laser-based or LED-based. Scanners that utilize lights with shorter wave lengths such as blue light produces more accurate scans than systems that uses longer wave lengths such as infrared light (Bluecam® compared with earlier generations of Cerec® intra-oral cameras) (8). Some scanners uses a collimating lens to convert the laser beam to a laser sheet (16). This laser sheet is expected to result in a faster scanning process compared to using a laser beam by capturing a wider area of the surface being scanned at once. Laser scanning technology is less affected by the ambient light compared to structured light scanning technology because the later uses the same range of light waves.(17)

One of the things that affects measuring accuracy of such systems is surface reflectivity of the scanned objects. Dusting the surface with antireflective powder is one of the ways that are currently used to overcome this problem (12).

Examples of scanners that uses the active triangulation principle are Bluecam® and Omnicam (Dentsply Sirona); and IOS FastScan™ (IOS Technologies Inc.). Bluecam® uses a 470 nm blue light and applies what is called active phase-shift triangulation by projecting a moving stripe pattern (alternating blue and black lines) across the tooth that moves four times in 0.16 second. The movement of stripe pattern across any point on the surface being scanned will cause a periodic shift in the intensity of the detected light (alternation between black and blue). This change in intensity is the key for calculating the surface depth information by using phase to

depth conversion algorithms that are based on triangulation (18, 19). Bluecam® is a still image system. This means the scanning wand should be held still during the scanning sequence.

Omnicaam®, in contrast to Bluecam®, projects light pattern with a different wave lengths (Figure 2) and is able to extract surface depth information from only one scan. It also has a short exposure time to counteract camera shake and allow free flowing high frame-rate imaging technique (1).

IOSs often combine more than one scanning technology. Examples of other technologies that are used beside triangulation are described next.

1.3.1.1 Polarizing multiplexer along with Scheimpflug imaging principle

IOS FastScan™ (IOS Technologies Inc.) intraoral scanner uses a polarizing multiplexer with two beam splitters at the scanner head to provide a configuration that combines the light from two object's perspectives, so to avoid the use of two cameras and hence result in a more compact design with reduced cost (16)

This scanner applies the Scheimpflug imaging principle. This principle allows one camera to capture in-focus images when the planes of the image, the lens and the object are not parallel. Alternatively, in-focus images can be still obtained according to the Scheimpflug principle when the three planes intersect in one point (Figure 3). This allows this type of intraoral scanner to capture the intraoral scene from two perspectives and accurately map the surface being scanned using active triangulation (12, 16, 20).

IOS FastScan™ has a camera that moves inside the wand and the operator has only to hold the wand in buccal, lingual and occlusal positions while scanning a full arch(12).

1.3.1.2 Active stereo-photogrammetry

Active stereo-photogrammetry is a technology that uses information from two or more 2D photos of objects obtained by a camera to construct 3D surface mapping of the surface being scanned by the aid of special algorithms (21, 22).

Parallax is the apparent displacement of an object from a distant background when viewed from different angles (Figure 4) (23). This principle is commonly used to estimate distances of objects in variety of fields including astronomy. It is based on viewing objects from two different angles and then using triangulation to calculate the distance of the object based on the amount of the apparent displacement.

MIA3d™ (Densys3D) IOS uses this technology. This scanner works by projecting 2D array of structured light on the intraoral scene as determined by the scanner's field of view. A first image is acquired at first angle (perspective) of the intraoral scene with the superimposed structured light pattern and stored. While the scanner is being moved a second image is acquired from a second angle (perspective) with the same superimposed structured light pattern. At least two images of the same intraoral scene from different perspectives are used by the scanner system. Matching features are identified from the obtained images of the same intraoral scene. A position calculator unit in the scanning wand calculates the relative 2D positions of the matched features relative to a reference created by projecting the same structured light pattern on a reference surface. After the relative position of the matching features are calculated for both the first and second angles(perspectives), a parallax of the matching feature points is calculated that will finally lead to identifying the 3D coordinate points of the scanned surface (22).

Scanners that uses photogrammetry are expected to moderately be less sensitive to the patient movement (12, 24). Factors affecting the accuracy of this type of scanning technology would be the camera resolution, zoom and number of photos taken by the scanner or what is called “photo redundancy”. The higher is the resolution, the better is the chance of identifying features more accurately and hence their location. Likewise, the higher number of perspective images that are taken, the more accurate is the reproduction of highly curved structures(25).

1.3.1.3 Active stereoscopic vision with structured light

Stereovision is a technology for 3D computer vision and extraction of 3D information from 2D scenes by the use of two calibrated cameras with known positions. This type of technology is based on the science of human vision (binocular vision: vision with two eyes). Humans are able to see and appreciate the depth of structures by the same principle; two images of the scene in sight with two different perspectives (angles) are projected on the retinas in a different location except part of the scene that lies at the intersection of line of sight of the two eyes. The visual cortex then processes this information that leads to 3D vision, or in other words, the perception of depth (Stereopsis) (12, 26). Likewise, active computer stereovision uses two calibrated cameras with known positions. In such stereoscopic vision systems, the centers of symmetry of the two camera lenses and the point of interest in the scanned object forms a triangle that is referred to as *Epipolar Plane* (Figure 5). Another concept that is important to help in understanding this technology is called binocular disparity. It is the shift in an image feature when viewed from two stereo images (taken from different perspective). A practical example of this is the apparent shift of an object when viewed using one eye while the other is closed then using the opposite eye while the other is closed. Disparity and distance of the scanned object

from camera are inversely related. The farther is the scanned surface point from the scanner, the less is the amount of disparity. This allows extraction of 3D coordinates from the 2D stereo images of the scanned surface using epipolar plane geometry described earlier and triangulation(26, 27).

Active stereovision uses a structured light projection to solve the problem of identifying common feature points from the two perspectives, also called correspondence problem, to allow for accurate calculation of the point coordinates. DirectScan intraoral scanner (HinT-Els) was based on this technology. This scanner captures images at an interval of 200ms and maps the intraoral scene by the use of computer software that performs pixel-precise comparisons (12, 27).

Bluescan®-I intraoral scanner (A●TRON3D® GmbH) is another example of scanner that uses active stereoscopic vision. (28).

1.3.2 Parallel Confocal Imaging Technique

This technology is based on the same technology applied in the confocal microscopy. It is based on a mechanism that collects only in-focus light reflected from the specimen and exclude out-of-focus light. iTero® (Align Technologies) IOSs are grounded on the this imaging technology. In brief, several parallel beams of laser light with known (x,y) coordinates are projected from a light source, which is located in the scanner head, towards the surface to be scanned at different focal planes. This is accomplished using focusing optics as a part of the lens assembly in the scanner system. The light intensity of the reflected light is detected by a charged coupled device (CCD) camera at various focal planes (in the z dimension) changeable by the scanner system. This CCD camera has a group of light sensing elements with each element representing a pixel in the image (x,y coordinates). A processor calculates spot-specific-position

(SSP) for each reflected light spot. This represents the focal plane (z dimension) at which the light spot yields the highest intensity (i.e. in-focus). The combination of the x-y-z coordinates of all the SSPs constitutes the 3D coordinates of the scanned surface. This scanner also captures color image information and projects real time colored 3D model on the screen while scanning (1, 12, 29).

3D progress (MHT) and TROIS™ (3Shape) are other examples of IOSs that implement parallel confocal imaging technology as a part of their image acquisition process.

Some of the different types of lens arrangements used in the 3D progress scanner lead to distortion of the scanned surfaces that are straight. But this seems to be totally manageable issue by computer processing because theoretical distortions are known and can be easily reproduced (12, 30).

1.3.3 Optical Coherence tomography

Optical coherence tomography can be explained as a cross-sectional imaging technique based on the property of light coherence. Coherent light waves are light waves that have the same frequency and have no phase difference, i.e. their peaks and valleys match (Figure 6). When two coherent light waves from a similar wave length meet they interfere and result in what is called “constructive interference” which is simply a wave with amplitude that equals the amplitude of both interfered waves (Figure 7). This constructive interference forms the basis of OCT scanners. It happens at a length called interference length that depends on bandwidth (range of frequencies) of the coherent light source used. For OCT, a low coherent light source is used; this means that constructive interference will happen only at short coherent length. This determines the axial resolution of OCT (31).

OCT based scanners split the light source to, a sample arm that is directed to the scanned object and to a reference arm that as directed to a reference mirror in the device that will reflect the light towards a photodetector (Figure 8). When the light in the sample arm is reflected back from the scanned object, it will be directed towards the photodetector too. When the total distance (also called time-of-flight) travelled by the sample light equals the distance travelled by the reference light they will both interfere and this interference pattern will be detected by the photodetector. It is also important to realize that the position of the reference mirror is changeable by a known value. This allows interference profile to be created from which a depth profile of the scanned surface is generated. Combining all the adjacent cross-sectional images will result in 3D mapping of the scanned surface(32).

The E4D Dentist's intraoral digitizer (E4D TECHNOLOGIES) uses a laser light source and applies the OCT technology. Moreover, the focusing optics, as was described in the patent of this scanner, may be designed in a way to serve as a confocal sensor by allowing changeable focusing position of the laser beam. This intraoral digitizer works by acquiring a series of images from fixed positions without the need of powder coating. 3D model is then constructed from the obtained single images (12, 33).

1.3.4 Active wavefront sampling

This type of scanning technology is based on a fundamental concept that was described by Federico Frigerio, "target feature's depth is encoded by the diameter of its defocus blur on the sensor plane". This basic principle has been well known by a full range of imaging technologies known as depth-from-defocus. In summary, if an object is situated in the focal plane of a camera, its image will be perfectly in-focus and the blur around it will be of zero magnitude. As the

object moves away from focal plane, the diameter of the blur increases in the resultant image. This diameter can be easily calculated by a known formula in optical geometrics. It is proportional to the distance of the object from the focal plane (Figure 9) (34).

Passive wave front sampling partially overcomes a disadvantage of traditional depth-from-defocus technologies that is represented by the difficulty of calculating the blur diameter from overlapping blur spots. It does so by providing a static sampling plane with two apertures that result in a two quasi-images of the target. This plane with two apertures is designed in a way that leads to a distance between features in the two quasi-images equal to the diameter of the blur and hence allows easier calculation (Figure 10). Adding more apertures will result in more sampling positions and greater accuracy of surface depth estimation, but this creates the problem of multiple overlapped images in objects with detailed features. A solution of that is to provide two static apertures and one rotating disc with specific aperture design (Figure 11) or to provide a rotating micro lens (Figure 12) . This leads to sampling clear single images that will appear rotating in a circular pattern; the diameter of this rotation will encode the depth information. The object features that are located farther away from the in-focus plane will have larger circular path (34). This technology is called active wavefront sampling (AWS).

True Definition intraoral scanner and the older generation Lava™ Chairside Oral Scanner (C.O.S) by 3M™ ESPE apply the AWS scanning technology along with blue stripe light projection using Blue LED lights. Lava C.O.S captures video at a rate of 20 3D datasets per second. This scanning technology used by the Lava C.O.S was described by manufacture as “3D-in-Motion technology”. This scanner requires the use of powder(12, 35).

1.4 Scanning technologies for IOSs under the stage of development

1.4.1 Accordion fringe interferometry

This scanning technology was developed at MIT Lincoln Laboratory based on the traditional linear laser interferometry. A 2D fringe light pattern that is produced by interference of two coherent lights from two different light sources is projected at the surface to be scanned (Figure 13). A digital camera at offset angle records the deformation of the projected pattern according to the contour of the surface. (36)

One of the important advantages of this technology is the inherent high dynamic range that enables the scan of dark and shiny surfaces without the need of powder application. Also this scanning technology is less sensitive to ambient light and its variations (12, 36).

DPI-3D scanner (Dimensional Photonics International) is based on the accordion fringe interferometry. This scanner has not reached the market yet but it has passed the prototype testing phase(12). The use of this technology for intraoral scanning is meant to eliminate the need for powder or to eliminate inaccuracies that result from different wavelength-dependent surface reflectivity and transmittance of enamel and dentine if no powder is used. Such difference in optical properties of enamel and dentine leads to inaccurate optical scanning of teeth due to incorporation of some subsurface areas instead of actual surface contours in the final 3D model of the dental structures(37). DPI-3D intraoral scanner uses two light sources that produce two coherent light beams with predetermined wavelengths. The scanner has the ability to detect light scattered from both surface and subsurface areas. A mechanism provides phase shift (Figure 14) of the light from one light source relative to the second one. Light reflected after the phase change from both surface and subsurface areas is detected. Three-dimensional position information is calculated according to reflectance detected before and after the phase shift(37).

1.4.2 Scanner based on Time-of-flight (TOF technology)

Time-of-flight scanners are used in the geographic and aerial scanning fields due to their high scanning speed. This scanning technology works by measuring the time needed for the light to reach the scanned object and reflect back to the scanner (19). Logozzo et al. introduced a prototype of intraoral scanner that is based on a two-channel pulsed time-of-flight (PTOF). This prototype achieved an average precision of $\pm 25 \mu\text{m}$ that seems adequate to be used in the dental field (38).

1.4.3 High frequency ultrasound 3D assisted micro-scanning

This non-optical technology is based on high frequency ultrasound (HFUS)-assisted micro-scanning. This promising technology was introduced to the intraoral scanning field by Heger et al(2). This technology has the ability to scan through the gingival tissue eliminating the need for retraction cord. Also it is less affected by moisture than optical scanning systems (2, 39, 40).

1.5 Accuracy of intraoral scanners

Accuracy of optical impressions in the dental literature is evaluated mainly by two methods. The first method is accomplished in-vitro on a sturdy dental model that is often fabricated from metal. This model is digitized with a reference (gold standard) scanner that has a validated accuracy to create a reference 3D model. An equivalent number of conventional and digital impressions are made for the dental model. Conventional impressions are digitized, either directly or indirectly after they are poured into stone, using the same reference scanner. Deviations of 3D models of each impression system from the reference are calculated after

superimposing (overlying) each model with the reference using special softwares that are specialized in measuring differences (41-45). This protocol allows the measurement of two variables that are used to define the accuracy of any measurement device according to ISO standard no. 5725-1:1994 (46). The two variables are, trueness and precision. Trueness represents mean deviation of a group of measurements from an original structure or a reference (45-47). Precision represents mean deviation between repeated measurement (43, 48). Higher trueness and precision are represented by lower value of those variables. For example, a measurement device that gives a mean deviation (error) of 10 μm from a reference value has less trueness than another device that gives a mean deviation of 5 μm from the same reference. On the other hand, a device that has a mean deviation of 10 μm between its repeated measurements is less precise than another device that has a mean deviation of 5 μm .

The second method of accuracy evaluation of optical impressions is by assessing marginal and internal fit of restorations fabricated using optical impressions compared to restorations obtained by conventional ones (49-51). This methodology evaluates the accuracy of the entire fabrication chain and not the impression system per se. This fabrication chain includes many error-prone steps starting from optical scanning and the associated 3D model creation processes, followed by all stages of restoration fabrication (e.g. Milling, 3D printing, casting) and post fabrication procedures (e.g. sintering, finishing and polishing). Therefore, the importance of the first protocol for evaluating the impression systems can't be overemphasized especially in the early stages of the development of new intraoral scanners or upgrading the existing ones.

Nevertheless, evaluating the accuracy of fit of dental restorations can't be ignored. It is important to measure the accuracy of restorations obtained by optical impressions, whether these

restorations are made using a complete digital workflow, or by including conventional manufacturing steps like waxing on physical model, casting, pressing, etc. However, the importance of this type of evaluation should come after the initial accuracy evaluation of the optical impression system itself.

The number of published studies evaluating the accuracy of optical impression systems is increasing rapidly reflecting the trend we are seeing towards digital dentistry. Comparing the results of the available studies is rather a difficult task due to differences in the study design, materials and scanners that are being evaluated. In addition, the technology of optical scanning is improving rapidly. However, we are seeing more studies every day with very close study design. This will help in building the evidence that is urgently needed for the dental practitioner and educational institutions to decide to what extent should this technology be incorporated in the daily dental practice and in the dental curriculum. A special focus will be given in this review and the coming manuscript to the accuracy of full-arch optical impressions. This is mandatory as the shift towards complete digital work flow is contingent on the ability of full-arch optical impressions to replicate oral and dental structures at a level of accuracy that at least equals that for conventional impressions.

Most of the studies pertaining to the subject of interest has evaluated accuracy in-vitro. All studies either measured trueness alone or both trueness and precision. Some of early studies used the terms trueness and accuracy interchangeably. Most of the authors used a very similar protocol to the one described earlier. However, they often used different devices, software packages and analyses methods.

Luthardt, Loos and Quaas compared trueness of a short span (three-teeth) optical impressions obtained by infrared-based intraoral scanner (Cerec® 3D camera, Sirona) to extra-

oral digitization of stone models poured from additional silicone (52). They reported lower accuracy of the intraoral scanner. The mean quadratic deviation (RMS) from reference was 27.9 μm and 18.8 μm for intraoral and extraoral digitization respectively. Prepared tooth areas showed deviations of almost half the magnitude of those at unprepared areas. This implies that the scanner used had some limitations in scanning complex tooth geometry compared to the simpler geometry of a tooth prepared for complete coverage crown.

Other study that evaluated longer span impressions by Mehl et al. found that quadrant impressions had more deviations than one tooth scans (35 μm compared to 19 μm) (53). They explained that by the accumulative effect of more inaccuracies being introduced in the final model while multiple single exposures are stitched together. However, their results showed 60% improvement in trueness of single-tooth impressions (Bluecam®) compared to an earlier intraoral scanner by the same manufacturer (Cerec 3D® camera). This confirmed the theoretical advantage of using visible blue light over a shorter wavelength infrared light in improving accuracy.

Several studies evaluated the accuracy of full-arch optical impressions in-vitro. Ender and Mehl compared accuracy of full-arch polyether impression and two optical impression systems (Lava™ COS, 3M™; Cerec Bluecam®, Sirona)(41). The authors used a reference scanner with high trueness and precision of $5.3 \pm 1.1 \mu\text{m}$ and $1.6 \pm 0.6 \mu\text{m}$ respectively. They concluded that optical impressions were comparable to polyether impressions. In a later study for the same authors, they used vinylsiloxanether® (VSXE®) (42). Their results showed that optical impressions represented by Bluecam® had significantly lower accuracy than conventional impressions, respectively, trueness and precision values of $58 \pm 15.8 \mu\text{m}$, $32 \pm 9.6 \mu\text{m}$ and $20.4 \pm 2.2 \mu\text{m}$, $12.5 \pm 2.5 \mu\text{m}$. They also reported accuracy being affected by different scanning protocols for

Bluecam® and Lava™ COS(43). On the other hand, Patzelt et al. reported a surprisingly huge difference in trueness and precision of Bluecam® compared to Lava™ COS and iTero (3Shape and Dentalwings) (54). The trueness for Bluecam® was $332 \pm 64.8 \mu\text{m}$ compared to a range of trueness between 38-49 μm for the other intraoral scanners used (54). The difference can't be explained only by different type of analysis they used. It could be due to systematic errors introduced by operator and powdering. Powder can be easily displaced when the scanner head hits the powdered tooth resulting in high deviations as was explained by Ender, Attin and Mehl (55).

In a recent study Ender and Mehl evaluated the accuracy of four different intraoral scanners compared to VSXE® and polyether impressions (47). They found that Bluecam® and VSXE® impressions have significantly higher trueness and precision than Omnicam (Sirona) , iTero (Cadent) and Lava™ COS. The VSXE® impressions showed homogeneous deviation across the arch not exceeding 20 μm except at the most distal teeth where deviation reached up to 50 μm . Omnicam and Bluecam® showed more deviations. Bluecam® showed a trend of maximum deviation appearing towards the most distal teeth in both sides, while Omnicam showing more prominent deviation at one distal side reaching up to 130 μm . iTero showed diagonal deviation extending from the premolar at one side to the molar on the opposite side. Lava showed irregular pattern of deviations that presented locally or across a complete quadrant. In this study Bluecam® showed significantly better trueness than Lava™ COS in a magnitude of approximately 14 μm . This result is opposite to an earlier study for the same authors using the same protocol (41). This might be due to software and hardware improvements in the Bluecam®, and more enhanced scanning protocol that was used by the authors in the later study. Software

version and hardware improvements was shown to affect intraoral scanner accuracy in another study(56).

Guth et al. reported higher trueness for direct digitization of 4-unit FDP preparation in-vitro with Lava™ COS compared to polyether impression and indirect digitization of stone models poured from polyether impressions (45). They reported trueness of 15.6 µm for Lava™ COS. Although they used a different type of analysis than what was used by Ender and Mehl, comparing results obtained by the two groups of authors shows that short-span optical impressions may be more accurate than full arch impressions (Trueness of 4-unit FDP impression was 15.6 µm compared to 40.3±14.1 µm for full-arch) (41, 45). This finding is in concordance with Giménez et al. in their in-vitro study that assessed the accuracy of optical implant impressions obtained by iTero(Cadent). They found that the length of the scan affected accuracy. Mean deviation between across arch implants was more than double the mean deviation of between same quadrant implants (53).

An interesting new in-vitro protocol for evaluating accuracy was introduced recently by Guth et. al that uses a metal bar that is connected to second molars across the arch. They measured the accuracy of the optical impressions by evaluating the linear accuracy of fit of captured bar ends that are extending from the two ends of the arch (Figure 15). The author suggested this protocol explaining that the superimposition protocol used by most of the authors is prone to analysis errors that increases as the size of the datasets increase which is the case in full arch impressions.

Available in-vivo studies evaluated only precision, obviously because reference scanner can't be used to perform intraoral scans. Flugge et al. tested the precision of intraoral (iTero, Align Technology) and extraoral digitization using the same scanner and lab scanner (D250,

3shape)(44). They found that intraoral digitization had the lowest mean precision value of 50 μm compared to extraoral digitization using the same scanner (25 μm) and using the lab scanner (10 μm). This study shows the significant effect of oral environment on the precision of optical impressions. Ender, Attin and Mehl found in their in-vivo study that VSXE® impressions had significantly higher precision than all the optical impression systems tested (Bluecam®, Omnicam, Lava™ COS, 3M™ True™ Definition, iTero, 3Shape Trios® and Trios® Color)(55). All scanners showed poorer precision than reported in-vitro precision. All optical impression systems didn't significantly differ between each other but had better precision than Alginate.

The trend of lesser accuracy with long-span impression can be clearly seen from the reviewed literature. Ender et al in a recent in-vivo study evaluated quadrant optical impressions compared to conventional full-arch and quadrant impressions (56). Quadrant optical impressions in this study showed better precision than full-arch impressions previously reported in a study by the same research group using the same protocol. Full-arch conventional impression in a metal tray showed the highest precision followed by True Definition, Trios® and Trios® Color with no significant differences between all groups. Most of the newer systems showed higher accuracy than older systems. This is probably due to hardware and software improvements. The authors reported that deviation patterns differed across the impression systems according to the scanning technology. Single-image systems showed higher deviations at the tooth surface while high-frame rate systems showed higher deviation at the gingival areas. Triple tray showed higher deviation at the occlusal areas. This is due to the decreased impression materials thickness at these areas. It is interesting to notice that all the intra-oral scanners used in this study had significantly higher precision than triple tray impressions expect iTero.

Time efficiency is an important factor especially in the private sector where it could be a critical factor in choosing the impression system. Grünheid, McCarthy & Larson reported faster alginate impressions that was also preferred by patients compared to intra-oral scanner (57). However, the difference was not significant between the two impression systems when they added post-impression processing time to the total time needed. It can be inferred from this that for diagnostic purposes, both impression systems might be equal in regard to total time consumption of the clinical staff.

1.6 Intraoral scanning challenges

3D optical scanning has been successful in many fields including dentistry. However, the intraoral environment is complex and creates challenges that all intraoral optical scanning technologies must overcome to produce accurate 3D mapping of dental structures.

Intraoral optical scanners depend on light reflection in its mechanism. The first challenge is the difference in optical properties of different substrates (teeth, prepared teeth, restorative materials and soft tissue)(12). Light reflection varies according to translucency parameter (TP) which is affected by object color and thickness. Different restorative materials have different TP, metallic restorations have zero TP and reflect the incident light directly while enamel allows light to penetrate its surfaces more than dentine (58). Powder application is meant to overcome this optical challenge. It has different purposes according to the scanning system used. One purpose is to act as antireflective on shiny surfaces that deflects light into direction different than the projected one and hence hinders the distance calculation of those shiny spots. A second purpose is to improve the accuracy of scanning by limiting the light reflection to 20 μm depth of the scanned tooth surfaces instead of highly variable depths rendered by translucent

tooth surfaces(59). The scanning depth is probably subject to change according to the powdering mechanism, material and scanning system used. Patzelt et al. stated that the purpose of powder in the lava C.O.S Intra-oral scanner is not to serve as antireflective, but its particles act as “connectors” to be joined through the scanning process (54). Powder-less Intraoral scanning systems must though overcome challenges imposed by translucent and reflective surface properties, otherwise it will result in far less accurate scans compared to those generated by powder systems.

The second biggest challenge is the humidity of the oral environment. It is of no wonder that saliva on the scanned surfaces creates artifacts during intraoral scan due to light refraction. This challenge is even harder for non-powder systems because it not as easy as the powdered surface to detect surface that has been wetted again after drying. The effect of wet surfaces is different according to the scanning technology. Triangulation, for example, is more sensitive to wet surfaces than confocal microscopy and time-of-flight methods (58). In a recent in-vitro study evaluating the effect of water on tooth surfaces scanned by Cerec® Omnicam, the authors found that 100 µm water film caused 25-35 µm measurement error according to the angle of the scanner against the surface(58).

The third challenge is the motion of the patient and the intraoral scanner. This requires short acquisition time to avoid blurry images in addition to Shake detection mechanism that permits still image acquisition (8, 12, 60).

Another challenge is scanning of sharp edges. This is known as “edge effects” which represent measurement errors that happen in from of roundation of sharp edges due to the limited camera resolution, or in form of spikes that may result in scanning systems that uses stripe pattern(Figure 16) . The later artifact is rare and limited to edges that are parallel to the stripe

pattern or at the buccal and lingual transitional lines. However it seems that this is manageable by the softwares and to some extent doesn't introduce critical fitting problems in the restorations (59).

Sensitivity of the scanning technology used to the ambient light is another challenge. This may require the headlight to be turned off and the operator to watch the screen while scanning. This might be challenging in the begging of the learning curve as it is hard to look only at the screen while scanning. looking at the scanner while scanning might be fatiguing to the eye due to the bright light produced by most of the scanners. Scanners that uses laser instead of structured light are less affected by the ambient light because the later uses light waves from the same range found in the ambient light(17).

Scanning time could be an issue in scanning full arch optical impressions. Most of the intraoral scanners allow enough time. This doesn't appear to be an issue once the operator gains enough experience in scanning.

Normal anatomical structures and limited mouth opening of some patients are also considered form the challenging factors in intraoral scanning. The proximity of the coronoid process of the mandible to the maxillary arch and the size of the scanning wand might complicate the scanning process at the distal end of the maxillary arch. In such situations, it may be beneficial to ask the patient to move the lower the jaw towards the side to be scanned.

Some systems require calibration due to the nature of the scanning technology and the nature of the scanner components. This calibration is often advised after first installation, shipment or other unusual conditions like big temperature changes. Failure to do this essential calibration procedure might affect the accuracy of the scanner.

Finally, it is worth to mention here how much is the need for reliable and smart softwares to support the scanning technology. Such softwares are able to implement sophisticated algorithms to stitch multiple exposures of the oral scene into one 3D model. The importance of such softwares to be able to detect scanning errors or artifacts and provide feedback to the user to provide the opportunity to rectify or patch the scan can't be overemphasized

CHAPTER 2: MANUSCRIPT

2.1 Introduction

Optical impressions can offer many advantages over conventional impressions. The optical impression has no dimensional change or susceptibility to damage from handling; needs less armamentarium (no need for trays, adhesives and dispensers); provides immediate on-screen feedback; increases the scope of planning and diagnosis; permits easier communication with the lab with no cross infection risk and allows easier duplication, storage and retrievability. Furthermore, it facilitates the fabrication of chairside definitive restorations (1). On the other hand, optical impressions have some limitations. The size of the scanning wand and the limited mouth opening may complicate scanning. Time limitation imposed by some systems might be problematic especially in the beginning of the learning curve. Moreover, it is difficult to scan subgingival margins.

Although the optical impression has impressive number of advantages, the adoption of this system in the daily dental practice and the shift towards complete digital flow are contingent on the ability of full-arch optical impressions to replicate oral and dental structures at a level of accuracy that is comparable to conventional impressions, or allow fabrication of restorations with a level of accuracy that is comparable to those obtained by conventional impressions.

Accuracy of optical impressions in the dental literature is evaluated mainly by two methods. The first method is accomplished in-vitro on a sturdy dental model that is often fabricated from metal. This model is digitized with a reference (gold standard) scanner that has a validated accuracy to create a reference 3D model. An equivalent number of conventional and digital impressions are made for the dental model. Conventional impressions are digitized, either

directly or indirectly after they are poured into stone, using the same reference scanner. Deviations of 3D models of each impression system from the reference are calculated after superimposing (overlying) each model with the reference using special softwares that is specialized in measuring differences (41-45). This protocol allows the measurement of two variables that are used to define the accuracy of any measurement device according to ISO standard no. 5725-1:1994 (46). The two variables are, trueness and precision. Trueness represents mean deviation (error) of a group of measurements from an original structure or a reference (45-47). Precision represents mean deviation between repeated measurement (43, 48). Higher trueness and precision are represented by lower value of those variables. For example, a measurement device that gives a mean deviation (error) of 10 μm from a reference value has less trueness than another device that gives a mean deviation of 5 μm from the same reference. On the other hand, a device that has a mean deviation of 10 μm between its repeated measurements is less precise than another device that has a mean deviation of 5 μm .

The second method of accuracy evaluation of optical impressions is by assessing marginal and internal fit of restorations fabricated using optical impressions compared to restorations obtained by conventional ones (49-51). This methodology evaluates the accuracy of the entire fabrication chain and not the impression system per se. This fabrication chain includes many error prone steps starting from optical scanning and the associated 3D model creation processes, followed by all stages of restoration fabrication (e.g. Milling, 3D printing, casting) and post fabrication procedures (e.g. sintering, finishing and polishing). Therefore, the importance of the first protocol for evaluating the impression systems can't be overemphasized especially in the early stages of the development of new intraoral scanners or upgrading the existing ones.

Most of studies that evaluated the accuracy of optical impression systems were performed in-vitro (41-43, 45, 52, 54). Available in-vivo studies evaluated only precision due to the fact that dental arches of research participants can't be scanned using reference scanner (44, 55, 56). However, there is a clear necessity of a protocol that evaluates both trueness and precision of full-arch optical impression in-vivo considering today's obvious trend towards digital dentistry. Therefore, the aim of this study was to introduce a protocol for evaluating both trueness and precision of full arch intra-oral optical impressions in-vivo. The Null hypothesis was that there is no difference in the mean trueness and precision of full-arch conventional and optical impressions in-vivo.

2.2 Materials and Methods

Five volunteers from UNC school of dentistry were enrolled in this study after IRB approval was received in August, 2014. Selection criteria were as following:

- Medically fit adult (18-50 years old).
- Angle's class I occlusion with no or mild crowding.
- No or few missing teeth.
- No TMJ problems or limitation of mouth opening.
- No symptoms of xerostomia and no medications that causes xerostomia.

An appliance was fabricated from Co-Cr RPD alloy for each participant. The appliance was designed in a way to fit over the occlusal surface the participant's mandibular teeth extending from first molar to first molar (Figure 17). This appliance was called "reference

appliance”. The purpose of this appliance was to facilitate trueness evaluation of the two impression systems in-vivo by:

- Providing a medium for in-vivo comparison. This is accomplished by obtaining both conventional and optical impressions for this appliance intraorally. On the other hand, each appliance will be scanned using a reference scanner to create reference 3D model to which both impression systems will be compared in the same way that was described earlier in the introduction. It basically replaces the dental model that was used in the previous in-vitro protocols.
- Providing a stiff medium of comparison that is resistant to any distortion during impression and disinfection procedures.

2.2.1 Reference appliance fabrication

Working model impression visit

Alginate substitute (*Silginat[®]; kettenbach, Huntington Beach, USA*) was used to obtain mandibular impressions. Impressions were disinfected (*CaviCide[™]; Metrex[™], Orange, USA*) and poured into type III dental stone (*Microstone; whipmix[®], Louisville, USA*).

Fabrication of reference appliances and special trays

Each reference appliance was fabricated first from light-cured acrylic custom tray material (*Triad[®] TruTray[™] VLC; Dentsply intenational, York, USA*). Impressions were kept after pouring the models and used as a matrix to replicate each participant’s dental anatomy. The stone model was used to fabricate the fitting surface of each appliance in a way to fit over the occlusal third of the participant’s teeth (Figure 18).

For each reference appliance, five special trays were fabricated with 4 millimeters spacer and 3 stoppers; one on the incisal edge of the lower right central incisor and the other two were behind the first molars in a seating channel specially designed to help orient the tray during impression procedure (Figure 19). The acrylic appliances were then digitized using CEREC[®] Omnicam (*Dentsply Sirona, Charlotte, USA*) intraoral scanner and sent for a RPD framework fabrication facility to be 3D printed into Co-Cr alloy (*3DRPD, Rouses Point, USA*) (Figure 20).

2.2.2 Obtaining impressions

All impression procedures were completed in two days. Five impressions using both impression systems (Conventional and optical) were obtained at the same visit for each participant by the same operator. Before the impression procedure, temperature record was obtained using infrared ear thermometer to exclude fever.

For better stability of the reference appliance during the impression procedures, a tray adhesive material was painted on the fitting surface and a rigid bite registration material was applied and the appliance was seated in the mouth. After complete set, the appliance was removed, excess was trimmed and separating medium was applied carefully to prevent impression material from sticking to the edges of the bite registration material during conventional impressions procedures.

All trays were painted with tray adhesive and kept at least 10 minutes to dry before loading with impression material. Reference appliance was kept in water bath over an inverted glass beaker to keep its temperature within one degree Celsius of the oral temperature as determined by infrared thermometer (Figure 21). After that, the appliance was placed intraorally and tray was loaded immediately with Vinylsiloxanether (VSXE[®]) impression material

(Identium[®]; Kettenbach, Huntington Beach, USA) and inserted over the appliance using the distal slot as guide for correct orientation.

All conventional impressions for each participant were obtained at room temperature and were allowed to set according to the manufacturer instructions (≥ 5 minutes and 30 seconds total working time). All impressions were checked for complete set before removal using periodontal probe to test complete rebound. After removal, each impression was checked for correct seating by looking for uniform material spread of the material around the appliance (Figure 22). The appliance was then removed using the distal extension provided to reduce any possible distortion. The appliance was then cleaned with rubbing alcohol to prepare it for the next impression.

Optical impressions were then obtained using CEREC[®] Omnicam (with CEREC SW 4.3 software). The reference appliance temperature was controlled before the first insertion using the water bath and was kept intraorally during successive impressions. Although Omnicam is a powder-less intraoral scanner, CEREC[®] Optispray (Dentsply Sirona, Charlotte, USA) was used lightly to help in scanning the reference appliance effectively due to the high reflectivity of its surface.

2.2.3 Creating reference models (Gold standards)

Impression storage and pouring

Conventional impressions were disinfected (CaviCide[™]) for 5 minutes and stored at room temperature then poured after 2 days by an experienced dental technician with a standardized powder /liquid ratio using low expansion type IV die stone (*Elite Rock, Zhermack, Badia Polesine, Italy*).

All reference appliances were lightly powdered with CEREC[®] Optispray (Figure 23) and scanned using a validated reference scanner (*Infinite focus standard; Alicona Corporation, Illinois, USA*) with trueness of $5.3 \pm 1.1 \mu\text{m}$ and precision of $1.6 \pm 0.6 \mu\text{m}$ (42). Reference 3D model for each reference appliance was generated (**Ref_n**, n=participant's ID). Due to the time consuming procedure and the limited availability of the reference scanner, four areas were selected from each reference appliance for comparison. These areas were the occlusal 1/3 of the right first molar, the lingual surface of the lower anterior teeth, the occlusal surface of the first premolar and the occlusal 1/3 of the left first molar (Figure 24).

All stone models were scanned using the reference scanner and digital models were generated too (**VSXE_{n-x}**, x=participant's ID, and x=impression no.). The same areas of comparison were selected.

Digital models were generated from optical impressions after they were uploaded to CEREC connect server and 3D models were obtained through CEREC inlab software (**Omni_{n-x}**).

2.2.4 Measuring deviations from reference models

3D models of the conventional and optical groups were initially aligned to their respective reference models (IF-Measure Suite 5.1, *Alicona Corporation, Illinois, USA*) and any areas outside the selected field of comparison were cropped out (Cloud Compare ver 2.6.2). Automatic fine alignment was performed afterwards (IF-Measure Suite 5.1). Any non-overlapped areas left after the second alignment were cropped out too (Cloud Compare) and imported back into the comparison software (IF-Measure Suite 5.1)(Figure 25). Deviations

between each impression and its respective reference model were then calculated using difference measurement module using “nearest” mode which calculates the mean absolute deviation between all the nearest signed neighbor points (trueness). This was done for all the impression replicates for each participant. This resulted in five trueness values for each participant. These values were then averaged for each participant and then averaged across all participants to give the total mean trueness for each impression system.

Precision for both groups was measured by calculating mean absolute deviations between all the possible pairs of impression replicates for each participant (1st to 2nd, 1st to 3rd ...etc. Total=10 pairs). The mean absolute deviations that were given as a result of this comparison constituted ten precision values for each participant. These values were then averaged for each participant and then averaged across all participants to give the total mean precision for each impression system.

All the data of each comparison was saved for further analysis. The numerical outputs of all comparisons were saved in an excel sheet. In addition, the deviations maps were saved for visual analysis of patterns of deviations (Figure 26).

2.3 Statistical analysis

Statistical analysis was performed using SAS® ver. 9.3 (*Cary, USA*). Separately by impression system, repeated measures ANOVA was used to assess whether there was a systematic difference in trueness or precision in the replicate measurements obtained for each impression. Using the averaged values for each impression, repeated measures ANOVA was used to assess whether the mean trueness and precision values differed across the two impression systems. Level of significance was set at 0.05.

2.4 Results

Trueness and precision values for the conventional impression group were consistently lower than those for the optical impression group across all participants. There was no statistically significant difference in the mean trueness and precision values across all participants for each impression systems alone (Table1).

The mean trueness for conventional impression and optical impression groups was $17.0 \pm 6.6 \mu\text{m}$ and $46.2 \pm 11.4 \mu\text{m}$ respectively. There was a statistically significant difference in the mean trueness between conventional and optical impression groups ($P = 0.01$). Percentiles for the trueness of each impression system were calculated and presented in a chart (Figure 27).

The mean precision for conventional and optical impression groups was $16.9 \pm 5.8 \mu\text{m}$ and $61.1 \pm 14.9 \mu\text{m}$ respectively. There was a statistically significant difference in the mean precision between conventional and optical impression groups ($P = < 0.01$). Percentiles for the precision of each impression system were also calculated and presented in a chart (Figure 28).

Regarding the pattern of deviation from reference models, conventional impressions group showed a uniform distribution of deviation across the area of comparison in 84% of the impressions. However, a band of higher deviation ranging between 80-140 μm appeared lingual to the central incisors in 16% of the impressions. Optical impressions group, on the other hand, showed clusters of bigger deviation at one or both molars in 88% of the impressions. The deviation was greatly prominent at either the left or right molar in 44% of the impressions (Figure 26). In these cases, deviation was $\geq 140 \mu\text{m}$ in 60% of the impressions and $> 250 \mu\text{m}$ in 28% of the impressions.

2.5 Discussion

While there are two methods for evaluating the accuracy of intraoral scanners in the dental literature, the interest of the authors was in the protocols that directly assess the accuracy of intraoral scanners and not the accuracy of fit of dental restorations obtained by optical impressions. The later protocol pertains to the accuracy of the whole fabrication chain and not the accuracy of the optical impression per se.

This study introduced a novel protocol for evaluating the accuracy (trueness and precision) of optical impressions in-vivo. This is the first study up to this moment that evaluated both trueness and precision intraorally. Several authors of in-vitro studies predicted that in-vivo accuracy of optical impression will be less than what is reported in-vitro due to the challenging nature of intraoral environment represented by moisture, restricted space and patient's movements (41, 42, 45, 54). Moreover, two in-vivo studies that evaluated precision confirmed the negative effect of the oral environment on the precision of optical impressions (44, 56).

In this study, conventional impressions showed significantly better trueness and precision than optical impressions. This finding was confirmed in in-vitro studies evaluating the accuracy (trueness and precision) of full-arch optical impressions (42, 47). However, the result of this study contradicted one of the earliest studies evaluating full-arch impressions by Ender and Mehl. They reported that both optical and conventional impressions were comparable (41). In that study they compared an optical impression system to polyether impression material which has lower accuracy than vinylsiloxane impression materials(61). However, the authors had a different conclusion when they compared the optical impression to the highly accurate VSXE® impression material (42). They concluded that full-arch optical impressions are less accurate than conventional impressions. They also confirmed that in another in-vitro study where they had

several optical impression systems compared to several conventional impression materials (VSXE®, polyether and Alginate)(47). In the later study they confirmed that the accuracy of full-arch polyether impressions was significantly less than VSXE® and some digital impression systems.

The findings of this study are comparable to other two in-vivo studies. Flugge et al. reported a significant effect of the intraoral environment when they compared the precision of direct intraoral digitization to indirect extraoral digitization of stone models using the same intraoral scanner (44). Ender, Attin and Mehl reported that all of the seven most popular optical impression systems they investigated showed decreased precision when they were used in-vivo (55) . They further explained that single-shot systems are more sensitive to patient, tongue and camera movement (due to inadequate support) than high frame rate capturing systems. They mentioned that softwares have the ability to detect to some extent artifacts that result from such movements and reject the scan so it can be repeated. They reported different precision results for two scanners from the same manufacturer but with different software versions.

The deviations of the conventional impressions from the reference models in this study were consistent across the area of comparison most of the time. On the other hand, the deviations of the optical impressions were mostly clustered at the distal molars with one of the sides being significantly more prominent than the other in almost half the impressions. These findings are comparable to the findings of two in-vitro and one in-vivo study (47, 54, 55). Moreover, in a recent in-vivo study by Ender et al., quadrant optical impressions obtained by three different intraoral scanners showed better precision than previously reported full-arch optical impressions and comparable to quadrant conventional impressions (56).

Unfortunately, until now there is no agreement on how much accuracy is needed for each clinical procedure. Acceptable marginal gap is another dilemma. It is ranging in the literature from 40 μm to less than 150 μm (62-66). It was shown in an in-vitro study that cement dissolution in crowns with 150 μm marginal gaps is significantly more than crowns with 25-75 μm gaps (66). Moreover, it is possible to achieve ≤ 50 μm marginal gap for gold castings and PFM crowns with or without porcelain butt joint, but this might be harder for milled crowns (62, 64). So the fabrication technique should be considered too. Anadioti et al. reported in an in-vitro study that best marginal fit was obtained by a combination of conventional VPS impression and pressed ceramic techniques(67). However, they also reported crowns obtained by a combination of optical impressions and either IPS e.max press or IPS e.max CAD produced clinically acceptable mean marginal accuracy ranging between 74-76 μm .

While there is disagreement in regard to the acceptable marginal gap, clinical success of single tooth restoration obtained by optical impressions has been reported in the literature (50, 68-70). A recent in-vivo study compared the fit of zirconia crowns obtained by intraoral digitization using three intraoral scanners compared to extraoral digitization of stone models using lab scanner. They found that marginal gaps of crowns obtained by optical impressions were comparable to the conventional ones except Omnicam(71). Also, several in-vitro studies reported that marginal and internal fit of 1-4 unit restorations obtained by optical impressions were comparable to those obtained by conventional impressions (51, 72, 73).

Digital technology is improving every day. We are witnessing rather rapid hardware and software improvements that are being applied in the field of optical impressions. A recent study reported that most of the newer intraoral scanning showed better precision than the older ones.

(56). We are expecting that optical impression systems will continue to improve and result in a more reliable full-arch impression for different treatment indications.

This study has several limitations. Although Omnicam is a powder-less intraoral scanner, a powder was necessary to overcome the high reflectivity of the polished metal. The appliances could have been sandblasted to lower their surface reflectivity, but it was decided to keep their surface smooth to prevent material residues from adhering on the surface in a way that may affect accuracy measurements. Also, had the surface been blasted, this could have introduced some errors due to the possible micro tears that might happen in the surface of the conventional impressions. On the other hand, powder application was light just to allow scanning. Had the powder possibly introduced serious deviations, areas of powder accumulation would have appeared consistently on subsequent optical impression replicates. However, each subsequent optical impression had different pattern of deviation although re-powdering was not performed between subsequent optical impressions except in few localized occasions at which it was carefully re-applied.

Another limitation is the use of metal appliance that is liable to some degree of thermal expansion and contraction. An effort to decrease the temperature fluctuation at the time of impression procedure was done by controlling the temperature of the appliance to within one degree Celsius before it was inserted intraorally. On the other hand, the reference scanner was in a room with controlled temperature during the time of scanning. So the effect of dimensional change was standardized across patients and across the impression systems.

The selection of only four areas to represent the whole arch has obviously prevented the authors from evaluating the pattern of deviation in the remaining areas of the arch. However, the smaller datasets that resulted from this selection may be in favor of decreasing the amount of

possible errors that might result from superimposing large datasets as was explained by Guth et al.(74).

The size of the appliance was limited to first molar- first molar. However, an appliance extending over the second molars was not possible using the presented design due to the limitation in the amount of comfortable mouth opening.

2.6 Conclusions

Within the limitation of this study:

1. The presented protocol for evaluating both trueness and precision in-vivo seems to be applicable.
2. Full-arch (first molar-first molar) optical impressions obtained by CEREC[®] Omnicam are less accurate than conventional VSXE impressions.
3. From the pattern of deviation that was observed to be more prominent in one of the quadrants, Omnicam may be accurate for quadrant impressions. Further research is needed to confirm that.

2.6 Future direction

Only one optical impression system was used in this study. It would be beneficial to apply this protocol using other available optical impression systems to allow comparison of the amount of in-vivo accuracy and the pattern of deviation obtained by different systems. Moreover; it would be helpful to explore a way to establish guidelines on much accuracy is required for each clinical procedure.

TABLES

Table 1 Mean trueness and precision for the conventional and optical impression groups.

ID	Trueness (mean \pm SD) μm		Precision (mean \pm SD) μm	
	Conventional	Optical	Conventional	Optical
1	21.1 \pm 8.9	36 \pm 13.4	22.4 \pm 7.5	55.2 \pm 24.2
2	17.8 \pm 4.6	38.6 \pm 13.7	18.9 \pm 3.0	43.6 \pm 20.7
3	10.5 \pm 1.5	63.2 \pm 19.2	10.9 \pm 2.3	83.0 \pm 35.0
4	25.3 \pm 7.3	52.9 \pm 8.9	21.7 \pm 3.8	56.5 \pm 16.1
5	10.4 \pm 0.9	39.5 \pm 10.7	10.7 \pm 1.2	67.4 \pm 32.7
P value	0.18	0.74	0.52	0.46

Table 2 Overall trueness and precision

Impression System	Trueness (mean \pm SD)	Precision (mean \pm SD)
Conventional	17.0 \pm 6.6	16.9 \pm 5.8
Optical	46.2 \pm 11.4	61.1 \pm 14.9
P Value	0.01	<0.01

FIGURES

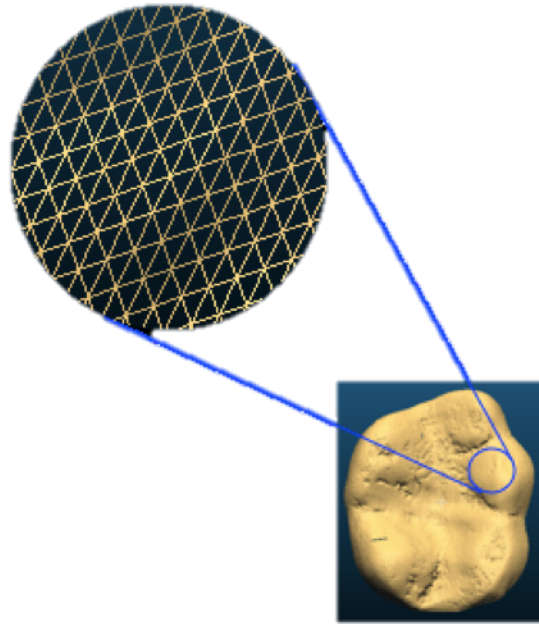


Figure 1. A zoomed-in view from a molar model showing 3D points connected in a form of triangles.



Figure 2. Omnicam stripe pattern.

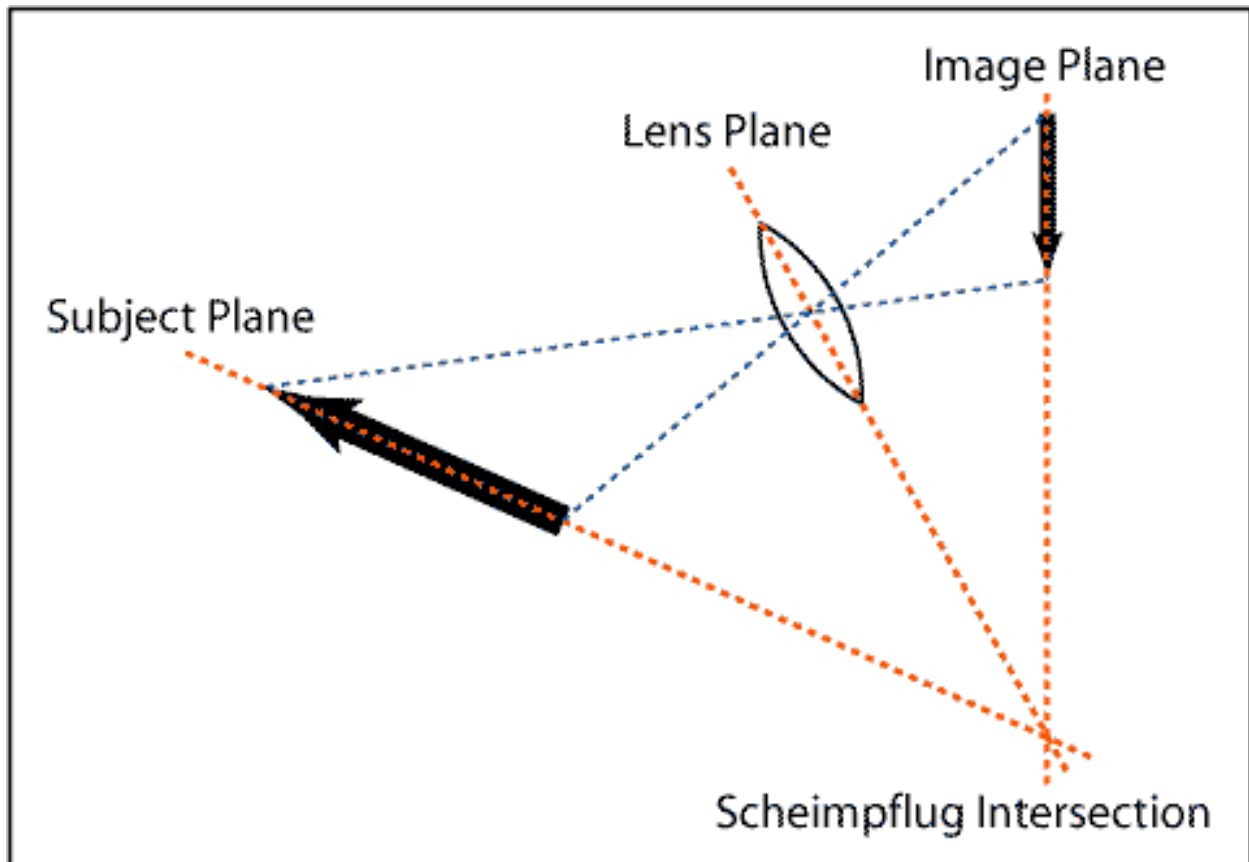


Figure 3. Scheimpflug principle. Three planes are intersecting into one point (Scheimpflug Intersection) (75).

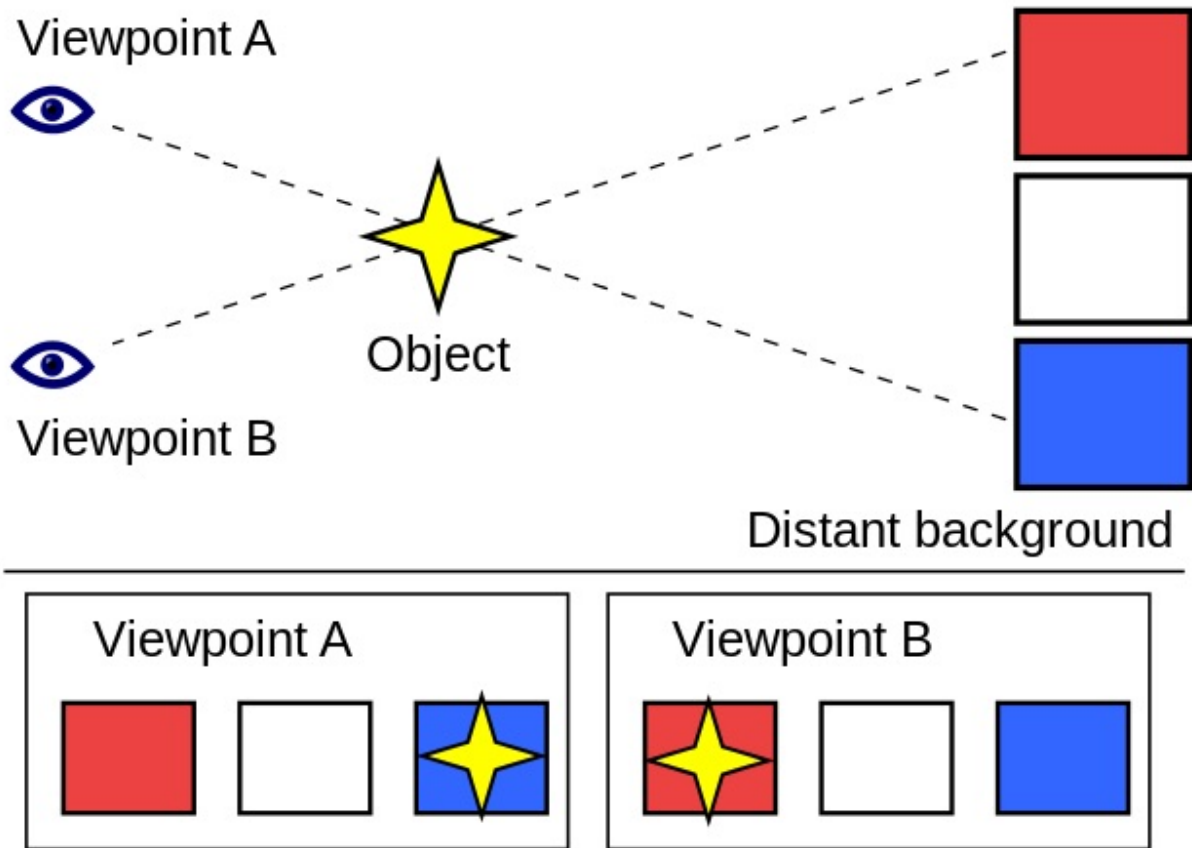


Figure 4. Representation of parallax by comparing the apparent position of the yellow star compared to the distant background when viewed from point A and B (23).

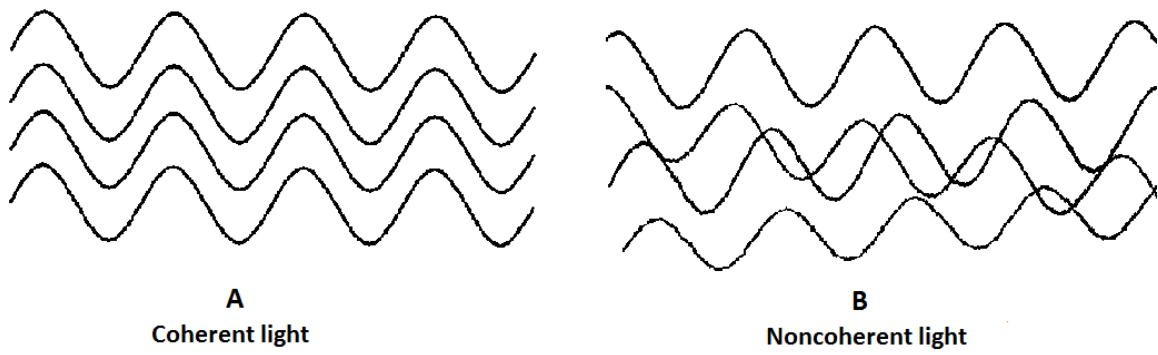


Figure 6. Coherent and non-coherent lights. (A) Coherent light with matching peaks and valleys (in-phase). (B) Noncoherent light with non-matching peaks and valleys (out of phase).

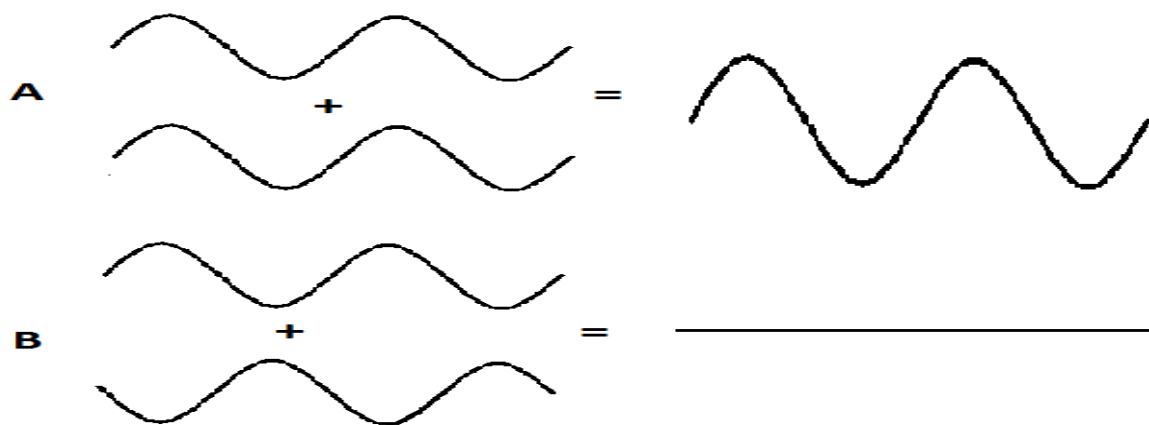


Figure 7. (A) Constructive interference (B) Destructive interference.

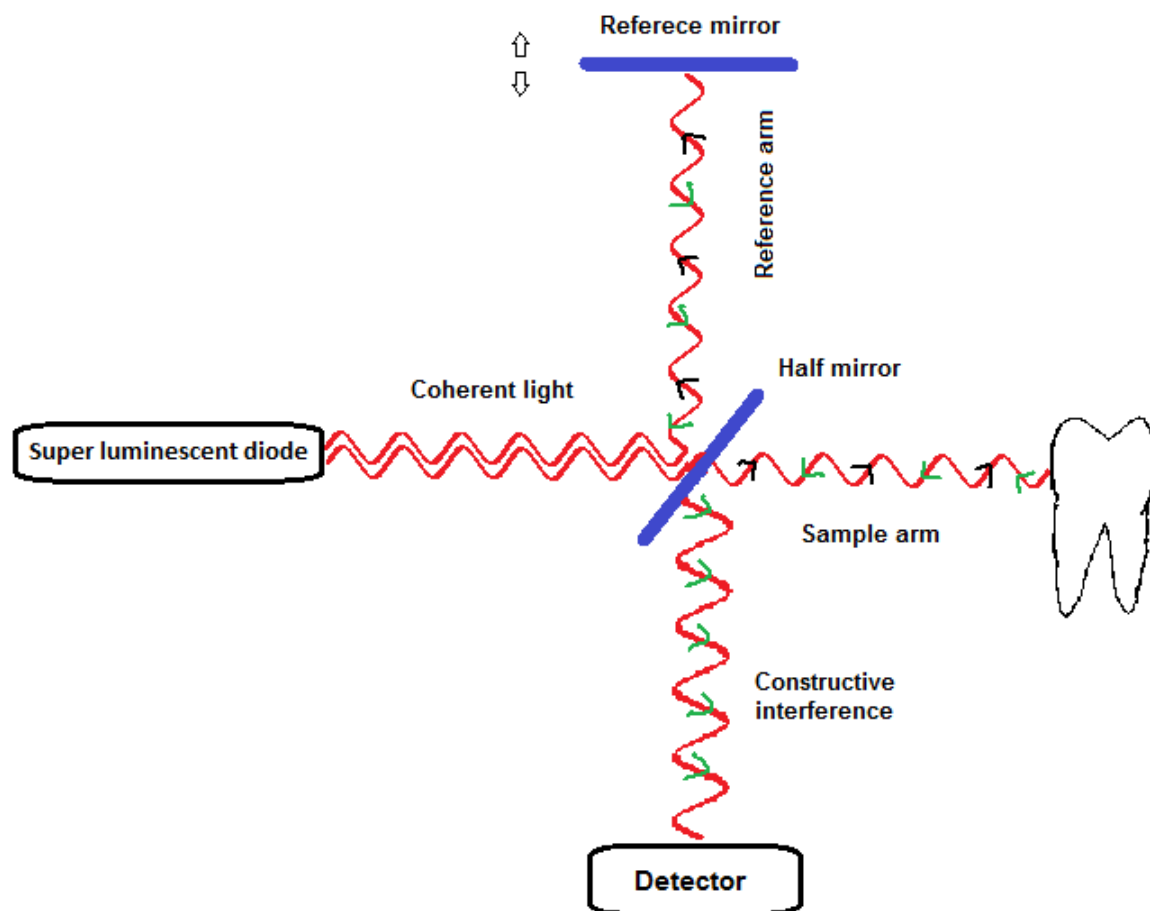


Figure 8. Schematic presentation of the OCT.

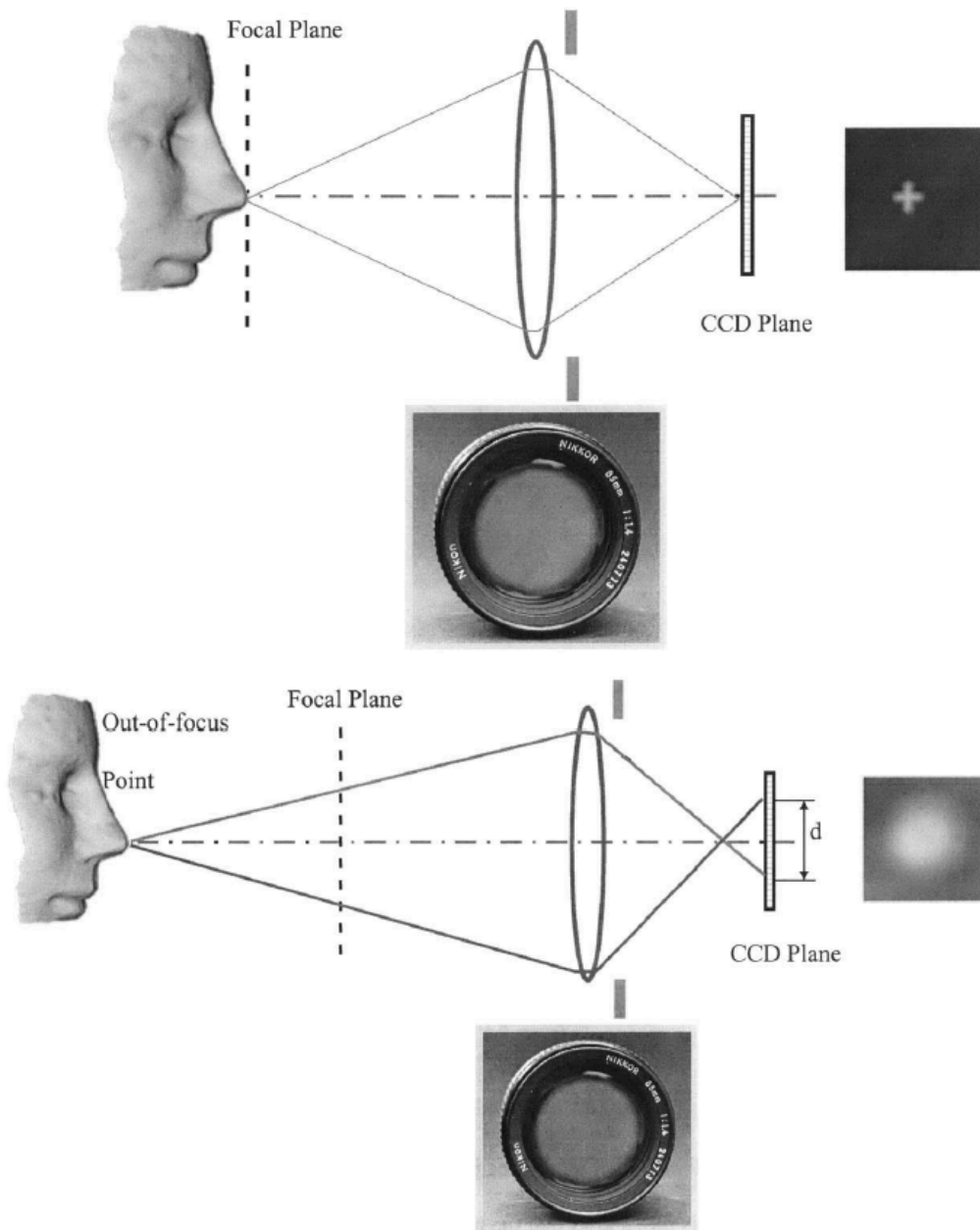


Figure 9. Schematic of depth-from-defocus approach. In top diagram, the target feature of interest is located on the lens in-focus plane. The feature's image is perfectly in focus and its blur spot diameter is effectively zero. In the bottom diagram, the target feature of interest is located some distance from the lens in-focus plane. The feature's image is out of focus, and the non-zero diameter of its blur spot is directly related to how far away the target is from the in-focus plane (77).

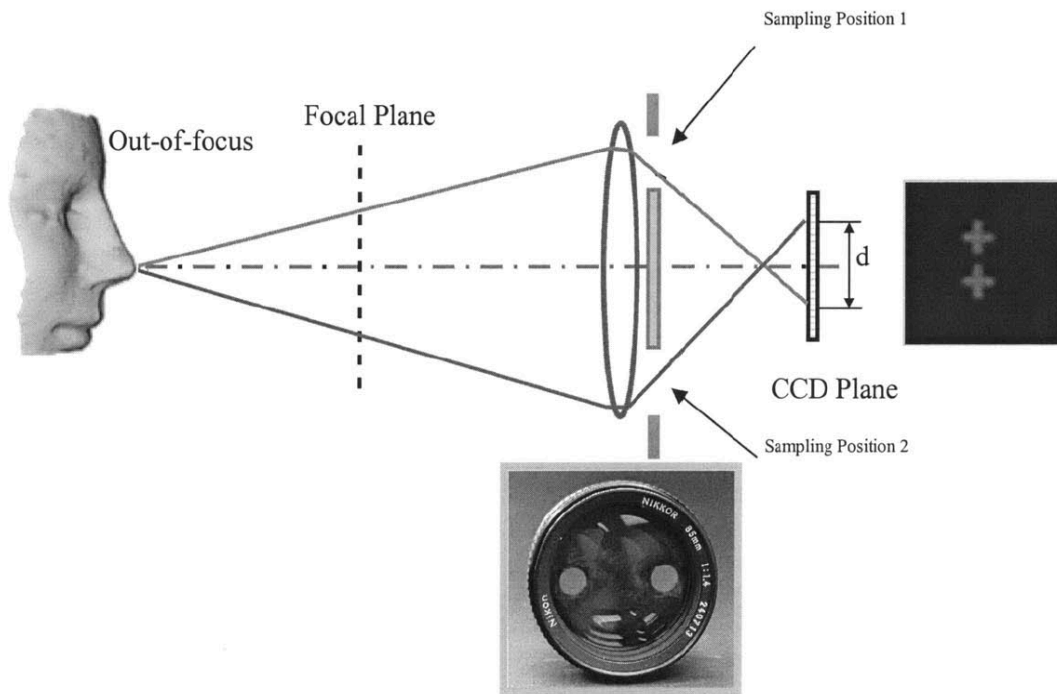


Figure 10. Static sampling of the wavefront with two diametrically opposed apertures separated by a distance equal to the overall aperture diameter in Figure 9. Instead of a defocus blur of diameter d , two quasi-focused images separated by the same distance d are recorded on the image plane (77).

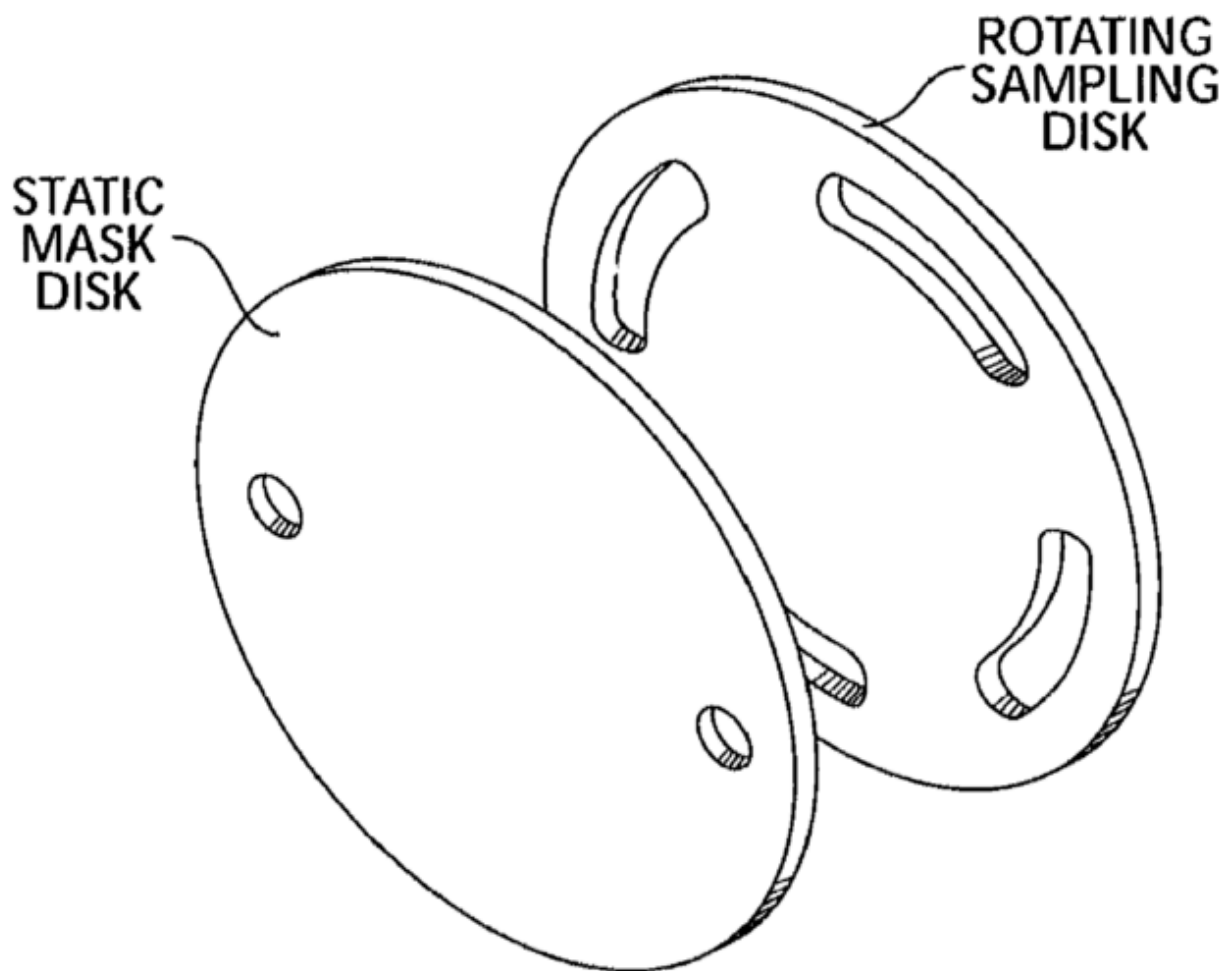


Figure 11. Static two apertures mask in conjunction with a rotating sampling disk (77).

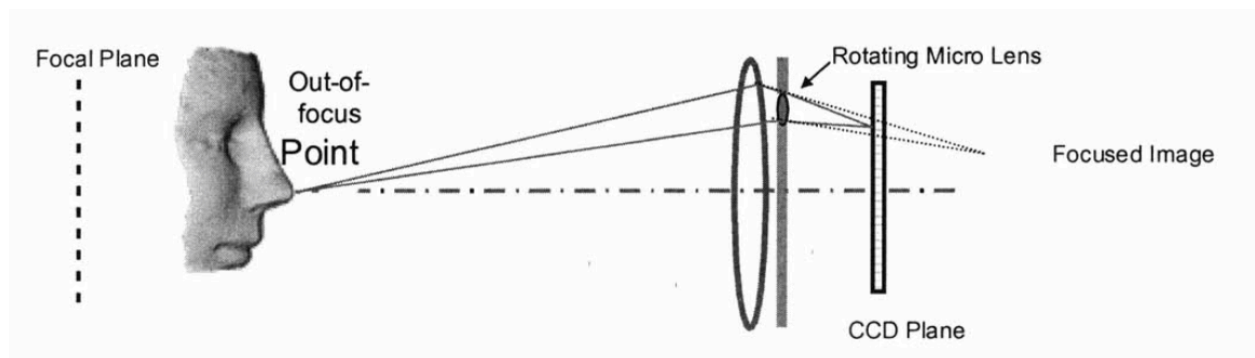


Figure 12. Microlense implementation in AWW (77).

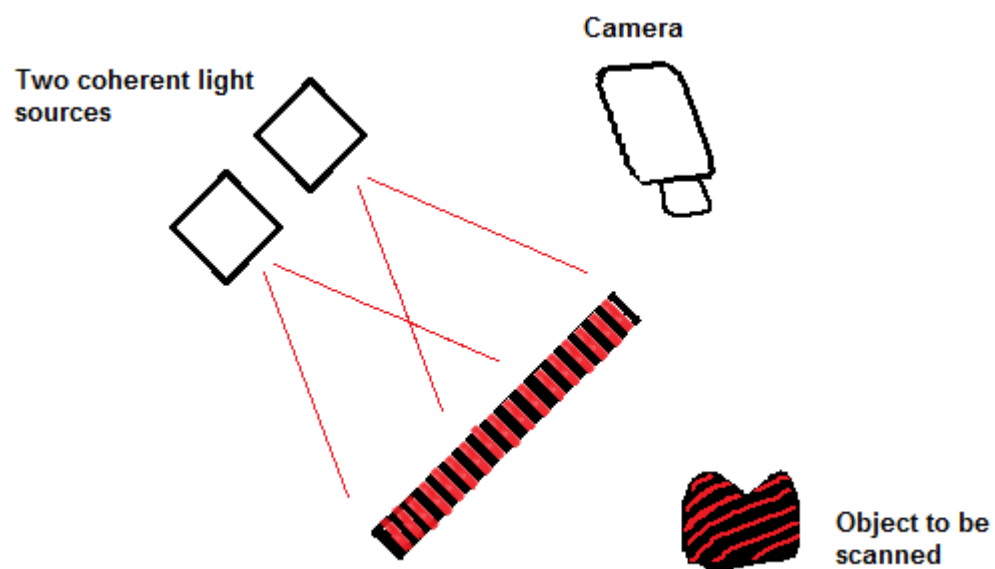


Figure 13. Schematic presentation of the Accordion Fringe Interferometry technology.

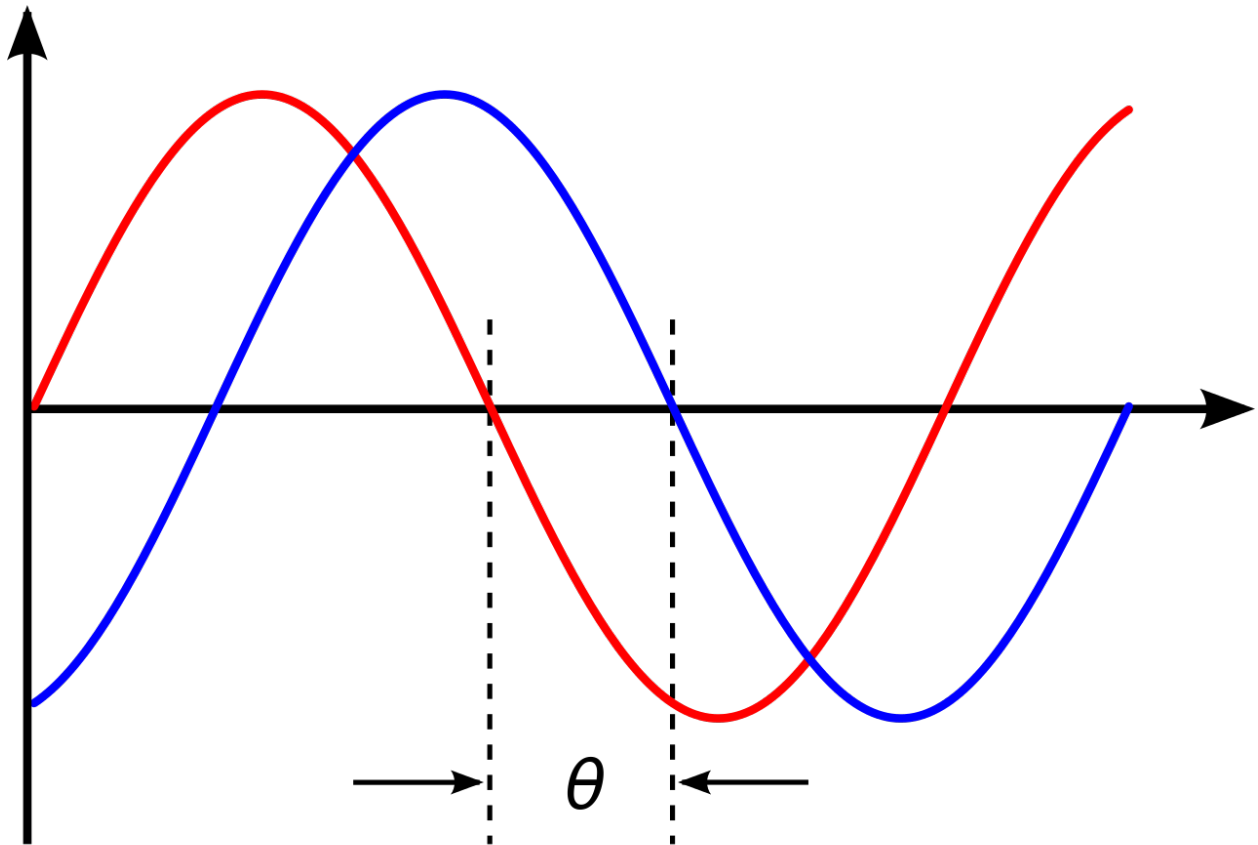


Figure 14. Illustration of phase shift. The horizontal axis represents an angle (phase) that is increasing with time (78).

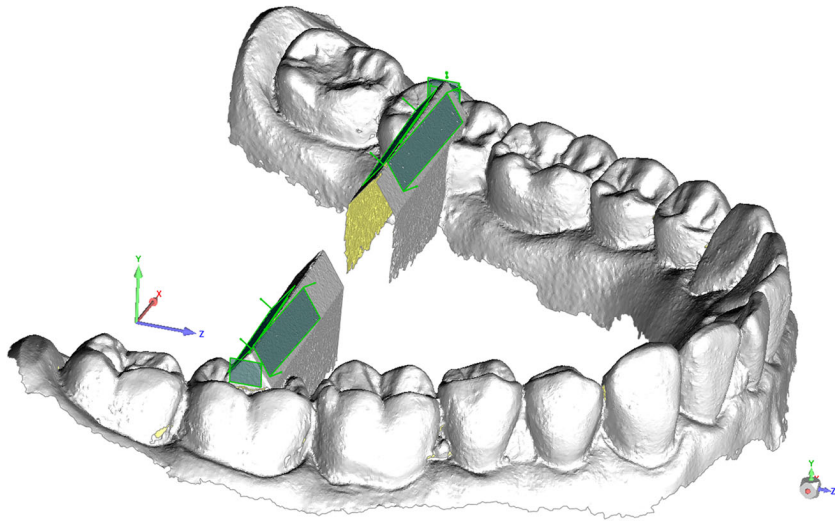


Figure 15. A new protocol for evaluating accuracy in-vitro by Guth et al. (74).

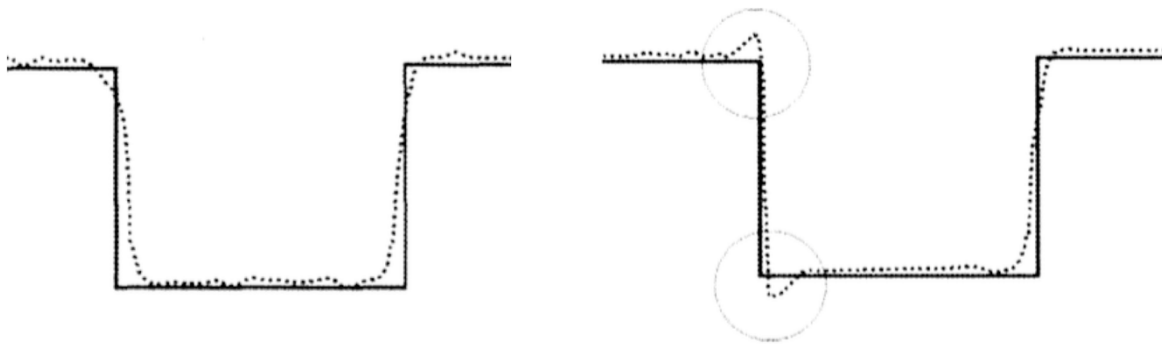


Figure 16. Edge effects (59).



Figure 17. Illustration of the reference appliance design.



Figure 18. Acrylic reference appliance.



Figure 19. Wax spacer over a reference appliance before tray fabrication.



Figure 20. Co-Cr reference appliance.



Figure 21. A reference appliance in the water bath to bring its temperature close to the oral temperature.



Figure 22. Conventional impression after excess was removed with scalpel.



Figure 23. A reference appliance powdered and ready for scan under the reference scanner.

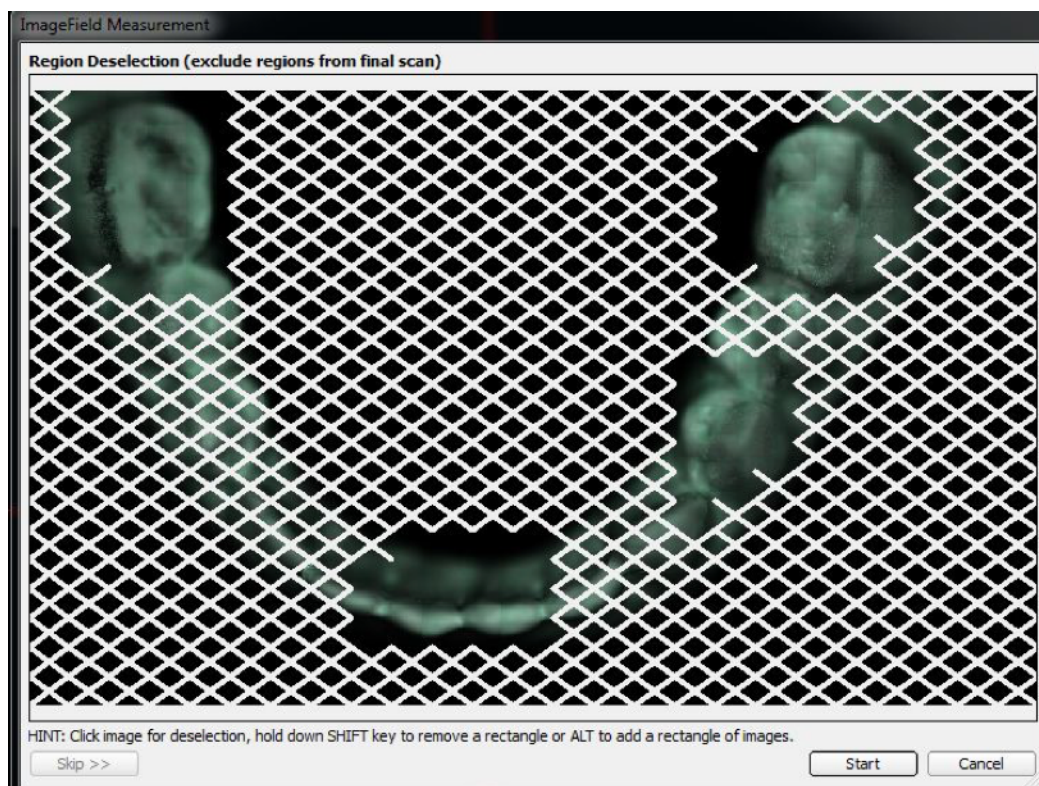


Figure 24. Image field selection before scanning with reference scanner.

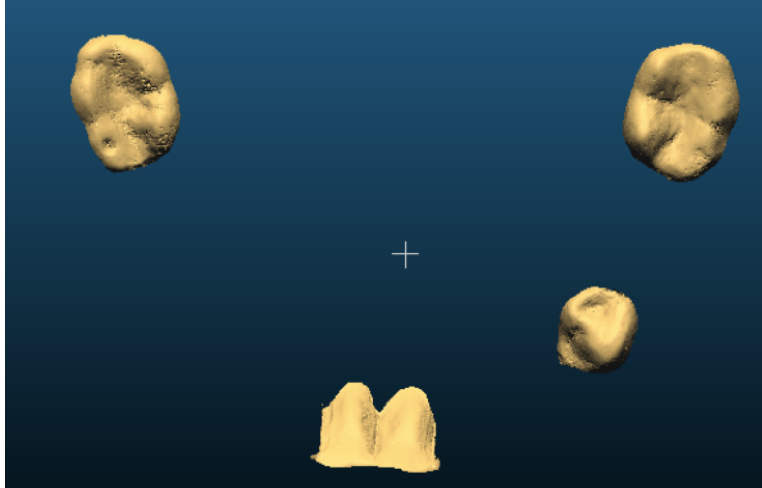


Figure 25. A cropped model after removing all the areas outside the field of comparison.

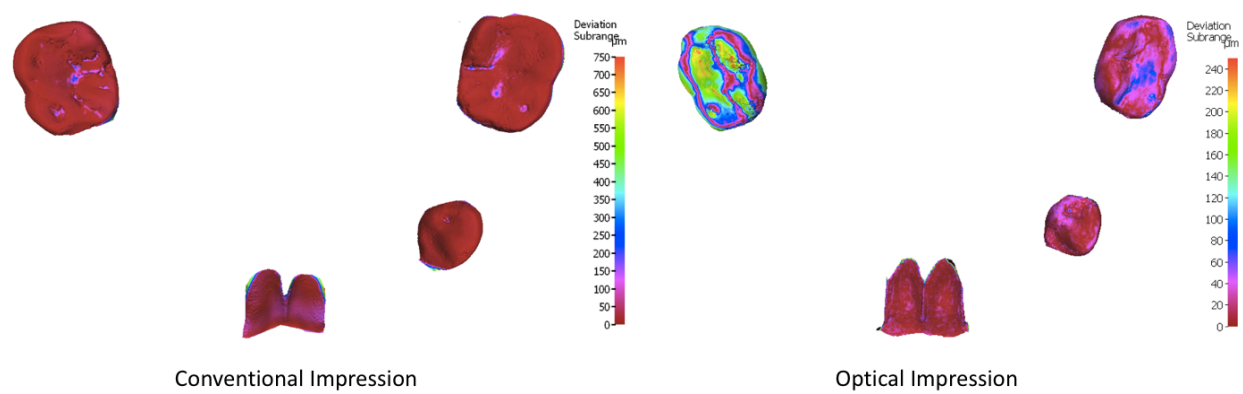


Figure 26. Example of the most common pattern of deviation from each impression system.

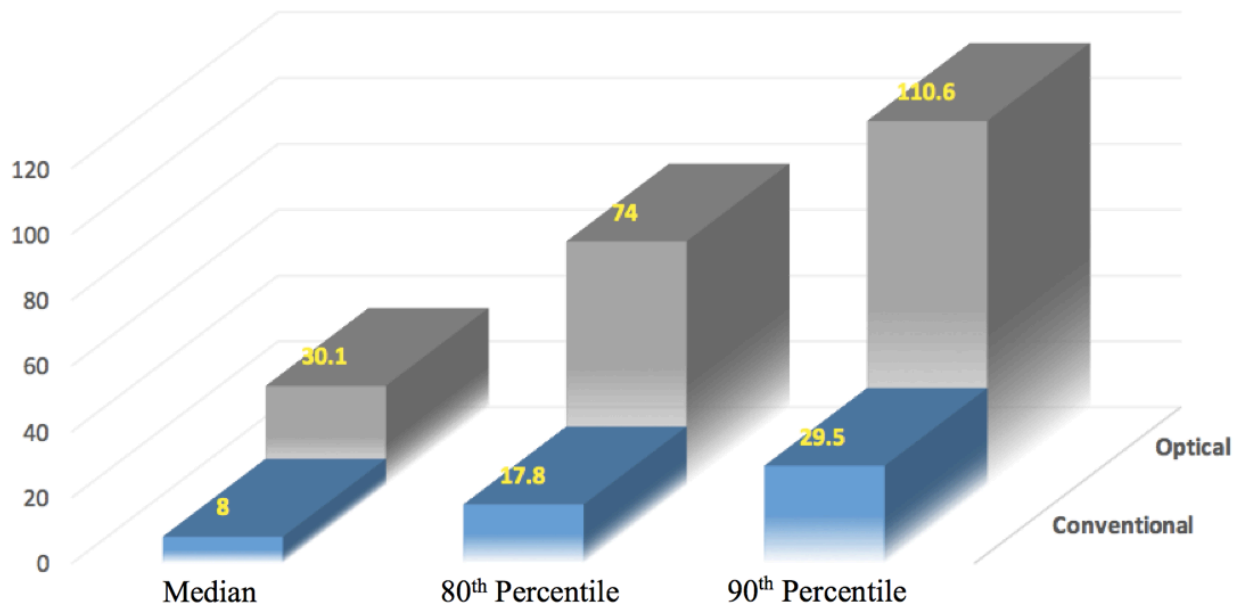


Figure 27. Distribution of trueness percentiles.

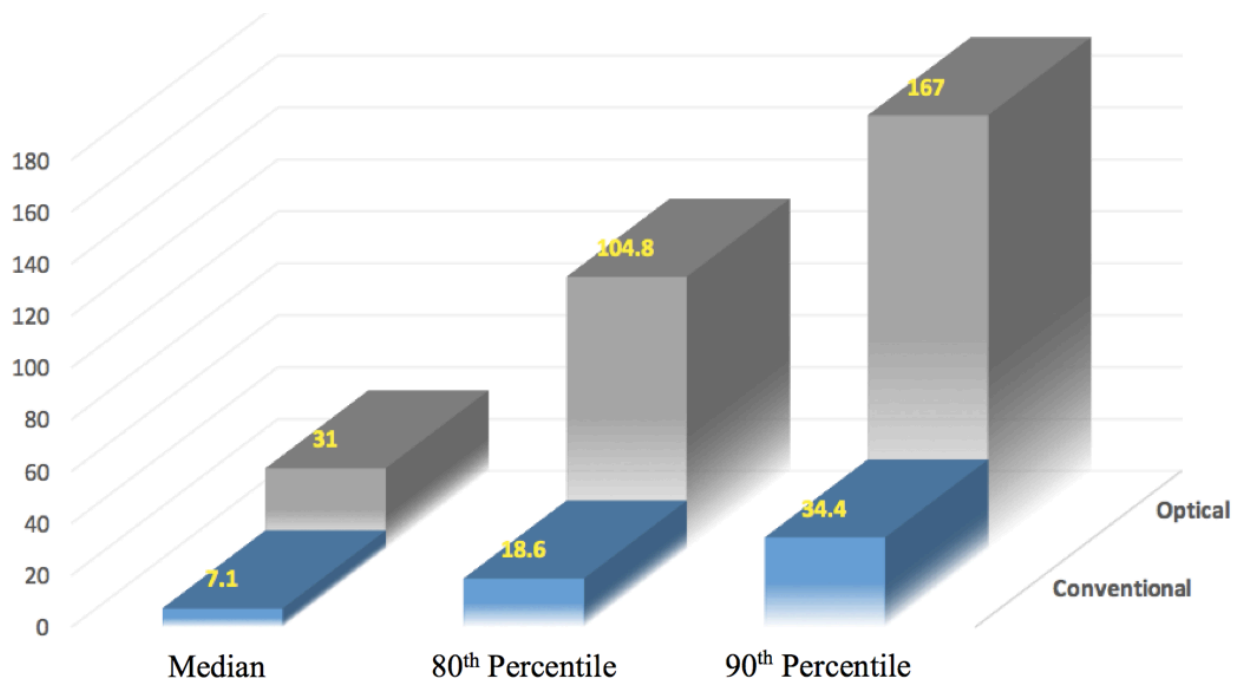


Figure 28. Distribution of precision percentiles.

REFERENCES

1. Reich S, Vollborn T, Mehl A, Zimmermann M. Intraoral optical impression systems--an overview. *International journal of computerized dentistry*. 2013;16(2):143-62.
2. Heger S, Vollborn T, Tinschert J, Wolfart S, Radermacher K, editors. Accuracy assessment of high frequency 3D ultrasound for digital impression-taking of prepared teeth 2013.
3. Khng KYK, Iowa Uo. An in vitro evaluation of the marginal integrity of CAD/CAM interim crowns compared to conventional interim resin crowns: University of Iowa; 2013.
4. Güth JFJ. Enhancing the predictability of complex rehabilitation with a removable CAD/CAM-fabricated long-term provisional prosthesis: a clinical report. *The Journal of prosthetic dentistry*. 107(1):1-6.
5. Yao JJ. Comparison of the flexural strength and marginal accuracy of traditional and CAD/CAM interim materials before and after thermal cycling. *The Journal of prosthetic dentistry*. 112(3):649-57.
6. Mehl A, Kunzelmann KH, Folwaczny M, Hickel R. Stabilization effects of CAD/CAM ceramic restorations in extended MOD cavities. *J Adhes Dent*. 2004;6(3):239-45.
7. Frankenberger R, Lohbauer U, Taschner M, Petschelt A, Nikolaenko SA. Adhesive luting revisited: influence of adhesive, temporary cement, cavity cleaning, and curing mode on internal dentin bond strength. *J Adhes Dent*. 2007;9 Suppl 2:269-73.
8. Logozzo AF, G.; Kilpelä, A.; Caponi, M.; Governi, L.; Blois, L. A Comparative Analysis Of Intraoral 3d Digital Scanners For Restorative Dentistry. *The Internet Journal of Medical Technology*. 2008;5(1).
9. Francois D. The optical Impression: University Claude-Bernard-Lyon; 1973.
10. Birnbaum NA, HB.; Stevens, C.; Cohen, B. . 3D Digital Scanners: A High-Tech approach to more accurate dental impressions. *inside Dentistry*. 2009;5.
11. Brunsvold MA, Lane JJ. The prevalence of overhanging dental restorations and their relationship to periodontal disease. *Journal of clinical periodontology*. 1990;17(2):67-72.
12. Logozzo S, Zanetti EM, Franceschini G, Kilpelä A, Mäkynen A. Recent advances in dental optics – Part I: 3D intraoral scanners for restorative dentistry. *Optics and Lasers in Engineering*. 2014;54:203-21.
13. Rudolph H, Luthardt RG, Walter MH. Computer-aided analysis of the influence of digitizing and surfacing on the accuracy in dental CAD/CAM technology. *Computers in biology and medicine*. 2007;37(5):579-87.

14. El-Hakim SF, Beraldin J-A, Blais F, editors. Comparative evaluation of the performance of passive and active 3D vision systems. Digital Photogrammetry and Remote Sensing'95; 1995: International Society for Optics and Photonics.
15. Whitty T. 3D Scanning 101. eLABORATE. 2010:46-8.
16. Trissel RG. Polarizing multiplexer and methods for intra-oral scanning. Google Patents; 2007.
17. Solutions EG. Scanning Technologies: Laser Light vs. Structured Light-based 2015 12/22/2015. Available from: [http://www.egsolutions.com/all/doc/upl/s1/technology/publications/Scanning technologies - laser light and structured light updated.pdf](http://www.egsolutions.com/all/doc/upl/s1/technology/publications/Scanning%20technologies%20-%20laser%20light%20and%20structured%20light%20updated.pdf).
18. Pfeiffer J. Dental CAD/CAM technologies: the optical impression (I). International journal of computerized dentistry. 1998;1(1):29.
19. Bellocchio F, Borghese NA, Ferrari S, Piuri V. 3D Surface Reconstruction electronic resource : Multi-Scale Hierarchical Approaches. New York, NY: Springer New York : Imprint: Springer; 2013.
20. Wikipedia contributors . Scheimpflug principle. Wikipedia [Internet]. 2015 23 December 2015. Available from: https://en.wikipedia.org/w/index.php?title=Scheimpflug_principle&oldid=680353686.
21. Wikipedia contributors. Photogrammetry. Wikipedia [Internet]. 2015 22 December 2015. Available from: <https://en.wikipedia.org/w/index.php?title=Photogrammetry&oldid=690701788>.
22. Ernst MM, Geffen M, Neta U, Cohen C. Three-dimensional modeling of the oral cavity. Google Patents; 2014.
23. Booyabazooka. An image showing an example of parallax.: Wikipedia; 2005.
24. Reece J. The pros and cons of photogrammetry vs. 3D Scanning for 3D printed figurines 2015 [Available from: <http://mcortechtechnologies.com/the-pros-and-cons-of-photogrammetry-vs-3d-scanning-for-3d-printed-figurines-blog/>].
25. Galantucci L, Percoco G, Ferrandes R. Accuracy issues of digital photogrammetry for 3D digitization of industrial products. Revue internationale d'ingénierie numérique. 2006;2(1-2):29-40.
26. Wikipedia contributors. Computer Stereo vision. Wikipedia [Internet]. 2015 27 December 2015. Available from: https://en.wikipedia.org/w/index.php?title=Computer_stereo_vision&oldid=693521897.

27. Wikipedia contributors.. Binocular disparity. Wikipedia [Internet]. 2015 28 December 2015. Available from:
https://en.wikipedia.org/w/index.php?title=Binocular_disparity&oldid=680474379.
28. Nowak C, Koinig H, JESENKO J. Device for recording images of three-dimensional objects. Google Patents; 2012.
29. Babayoff N, Glaser-Inbari I. Imaging a three-dimensional structure by confocal focussing an array of light beams. Google Patents; 2004.
30. Berner M. Optical System for a Confocal Microscope. Google Patents; 2010.
31. Drexler W, Fujimoto JG. Optical Coherence Tomography: Technology and Applications: Springer Berlin Heidelberg; 2008.
32. Huang D, Swanson EA, Lin CP, Schuman JS, Stinson WG, Chang W, et al. Optical Coherence Tomography. Science. 1991;254(5035):1178-81.
33. Quadling H, Quadling M, Blair A. Laser digitizer system for dental applications. Google Patents; 2007.
34. Frigerio F. 3-dimensional surface imaging using Active Wavefront Sampling [Thesis]: Massachusetts Institute of Technology; 2006.
35. 3M™ True Definition Scanner Frequently Asked Questions.: 3M Oral Care; 2015.
36. Bloss R. Accordion fringe interferometry: a revolutionary new digital shape-scanning technology. Sensor Review. 2008;28(1):22-6.
37. Dillon RF, Zhao B, Judell NHK. Intra-oral three-dimensional imaging system. Google Patents; 2009.
38. Logozzo S, Kilpelä A, Mäkynen A, Zanetti EM, Franceschini G. Recent advances in dental optics – Part II: Experimental tests for a new intraoral scanner. Optics and Lasers in Engineering. 2014;54:187-96.
39. Chuembou Pekam F, Marotti J, Wolfart S, Tinschert J, Radermacher K, Heger S. High-frequency ultrasound as an option for scanning of prepared teeth: an in vitro study. Ultrasound in medicine & biology. 2015;41(1):309-16.
40. Vollborn T, Habor D, Pekam FC, Heger S, Marotti J, Reich S, et al. Soft tissue-preserving computer-aided impression: a novel concept using ultrasonic 3D-scanning. International journal of computerized dentistry. 2014;17(4):277-96.
41. Ender A, Mehl A. Full arch scans: conventional versus digital impressions--an in-vitro study. International journal of computerized dentistry. 2011;14(1):11-21.

42. Ender A, Mehl A. Accuracy of complete-arch dental impressions: a new method of measuring trueness and precision. *The Journal of prosthetic dentistry*. 2013;109(2):121-8.
43. Ender A, Mehl A. Influence of scanning strategies on the accuracy of digital intraoral scanning systems. *International journal of computerized dentistry*. 2013;16(1):11-21.
44. Flugge TV, Schlager S, Nelson K, Nahles S, Metzger MC. Precision of intraoral digital dental impressions with iTero and extraoral digitization with the iTero and a model scanner. *American journal of orthodontics and dentofacial orthopedics : official publication of the American Association of Orthodontists, its constituent societies, and the American Board of Orthodontics*. 2013;144(3):471-8.
45. Guth JF, Keul C, Stimmelmayer M, Beuer F, Edelhoff D. Accuracy of digital models obtained by direct and indirect data capturing. *Clinical oral investigations*. 2013;17(4):1201-8.
46. Normung DDIf. Accuracy (trueness and precision) of measurement methods and results -- Part 1: General principles and definitions (ISO 5725-1:1994).
47. Ender A, Mehl A. In-vitro evaluation of the accuracy of conventional and digital methods of obtaining full-arch dental impressions. *Quintessence Int*. 2015;46(1):9-17.
48. Ziegler M. Digital impression taking with reproducibly high precision. *International journal of computerized dentistry*. 2009;12(2):159-63.
49. Almeida ESJS, Erdelt K, Edelhoff D, Araujo E, Stimmelmayer M, Vieira LC, et al. Marginal and internal fit of four-unit zirconia fixed dental prostheses based on digital and conventional impression techniques. *Clinical oral investigations*. 2013.
50. Syrek A, Reich G, Ranftl D, Klein C, Cerny B, Brodesser J. Clinical evaluation of all-ceramic crowns fabricated from intraoral digital impressions based on the principle of active wavefront sampling. *Journal of dentistry*. 2010;38(7):553-9.
51. Tidehag P, Ottosson K, Sjogren G. Accuracy of Ceramic Restorations Made Using an In-office Optical Scanning Technique: An In Vitro Study. *Operative dentistry*. 2013.
52. Luthardt RG, Loos R, Quaas S. Accuracy of intraoral data acquisition in comparison to the conventional impression. *International journal of computerized dentistry*. 2005;8(4):283-94.
53. Mehl A, Ender A, Mormann W, Attin T. Accuracy testing of a new intraoral 3D camera. *International journal of computerized dentistry*. 2009;12(1):11-28.
54. Patzelt SB, Emmanouilidi A, Stampf S, Strub JR, Att W. Accuracy of full-arch scans using intraoral scanners. *Clinical oral investigations*. 2014;18(6):1687-94.
55. Ender A, Attin T, Mehl A. In vivo precision of conventional and digital methods of obtaining complete-arch dental impressions. *The Journal of prosthetic dentistry*. 2015.

56. Ender A, Zimmermann M, Attin T, Mehl A. In vivo precision of conventional and digital methods for obtaining quadrant dental impressions. *Clinical oral investigations*. 2015;1-10.
57. Grunheid T, McCarthy SD, Larson BE. Clinical use of a direct chairside oral scanner: an assessment of accuracy, time, and patient acceptance. *American journal of orthodontics and dentofacial orthopedics : official publication of the American Association of Orthodontists, its constituent societies, and the American Board of Orthodontics*. 2014;146(5):673-82.
58. Kurz M, Attin T, Mehl A. Influence of material surface on the scanning error of a powder-free 3D measuring system. *Clinical oral investigations*. 2015;19(8):2035-43.
59. Pfeiffer J. Dental CAD/CAM technologies: the optical impression (II). *International journal of computerized dentistry*. 1999;2(1):65-72.
60. Mehl A. 2009--the quantum leap for intraoral optical measurement? *International journal of computerized dentistry*. 2009;12(1):3-5.
61. Balkenhol M, Ferger P, Wostmann B. Dimensional accuracy of 2-stage putty-wash impressions: influence of impression trays and viscosity. *Int J Prosthodont*. 2007;20(6):573-5.
62. Christensen GJ. Marginal fit of gold inlay castings. *Operative dentistry*. 1966;16(2).
63. McLean JW, von Fraunhofer JA. The estimation of cement film thickness by an in vivo technique. *British dental journal*. 1971;131(3):107-11.
64. Belser UC, MacEntee MI, Richter WA. Fit of three porcelain-fused-to-metal marginal designs in vivo: a scanning electron microscope study. *The Journal of prosthetic dentistry*. 1985;53(1):24-9.
65. Fransson B, Oilo G, Gjeitanger R. The fit of metal-ceramic crowns, a clinical study. *Dental materials : official publication of the Academy of Dental Materials*. 1985;1(5):197-9.
66. Jacobs MS, Windeler AS. An investigation of dental luting cement solubility as a function of the marginal gap. *The Journal of prosthetic dentistry*. 1991;65(3):436-42.
67. Anadioti E, Aquilino SA, Gratton DG, Holloway JA, Denry I, Thomas GW, et al. 3D and 2D Marginal Fit of Pressed and CAD / CAM Lithium Disilicate Crowns Made from Digital and Conventional Impressions. 2014:1-8.
68. Reiss B. Clinical results of Cerec inlays in a dental practice over a period of 18 years. *International journal of computerized dentistry*. 2006;9(1):11-22.
69. Reiss B, Walther W. Clinical long-term results and 10-year Kaplan-Meier analysis of Cerec restorations. *International journal of computerized dentistry*. 2000;3(1):9-23.

70. Otto T, De Nisco S. Computer-aided direct ceramic restorations: a 10-year prospective clinical study of Cerec CAD/CAM inlays and onlays. *Int J Prosthodont*. 2002;15(2):122-8.
71. Boeddinghaus M, Breloer ES, Rehmann P, Wöstmann B. Accuracy of single-tooth restorations based on intraoral digital and conventional impressions in patients. 2015.
72. Seelbach P, Brueckel C, Wostmann B. Accuracy of digital and conventional impression techniques and workflow. *Clinical oral investigations*. 2013;17(7):1759-64.
73. Svanborg P, Skjerven H, Carlsson P, Eliasson A, Karlsson S, Ortorp A. Marginal and internal fit of cobalt-chromium fixed dental prostheses generated from digital and conventional impressions. *International journal of dentistry*. 2014;2014:534382.
74. Guth JF, Edelhoff D, Schweiger J, Keul C. A new method for the evaluation of the accuracy of full-arch digital impressions in vitro. *Clinical oral investigations*. 2015.
75. Hunter F. Scheimpflug. Wikipedia; 2006.
76. Nordmann A. Epipolar Geometry. Wikipedia; 2007. p. Epipolar geometry.
77. Frigerio F. Passive Wave Front Sampling. Massachusetts Institute of Technology; 2006.
78. Peppergrower. Two sinusoidal waves offset from each other by a phase shift θ .: Wikipedia; 2009.